Chapter 2
Development of a Mirror-Image Screening System for Chiral Natural Products

Abstract In this section, a novel approach for identifying MDM2-p53 and MDMX-p53 protein–protein interactions (PPIs) inhibitors by using chemically synthesized MDM2 and MDMX proteins has been established. MDM2 and MDMX are oncoproteins that negatively regulate the activity and stability of the tumor suppressor protein p53. The inhibitors of PPIs of MDM2-p53 and MDMX-p53 represent potential anticancer agents. Affinity-based chemical array screening is one of the efficient methods for identification of binding agents toward various pockets of proteins. To establish chemistry-based screening platform for identification of MDM2 and MDMX inhibitors, synthetic strategy of MDM2 and MDMX proteins and application of these proteins for chemical array screening were performed. MDM2 and MDMX proteins were prepared by Fmoc-based solid-phase peptide synthesis (SPPS), and binding candidates for them were identified from an in-house compound library by chemical array screening. The subsequent fluorescence polarization (FP) assay identified peptidic compounds that inhibited MDM2-p53 and MDMX-p53 interactions.

Keywords MDM2/MDMX proteins · Chemical protein synthesis · Chemical array screen · Mirror-image protein technology · Natural products-based drug discovery

2.1 Establishment of Screening Process Using Synthetic MDM2 and MDMX Proteins

MDM2 and MDMX are negative regulators of the tumor suppressor protein p53, and therefore confer tumor development and survival [1]. MDM2 and MDMX bind to the N-terminal transactivation domain of p53 with high affinity to inhibit functions associated with regulating responsive gene expression [2]. MDM2 has E3 ubiquitin ligase activity and thus also regulates the stability of p53 by proteasomal degradation, thereby conferring effective down-regulation of cellular p53 protein levels [3]. MDMX has no ubiquitin ligase activity, yet forms a MDMX-MDM2 heterodimer via interaction between their C-terminal RING finger domains. This heterodimer stimulates MDM2-mediated ubiquitination of the p53 and subsequent degradation

© Springer Nature Singapore Pte Ltd. 2018

T. Noguchi, *Development of Chemistry-Based Screening Platform for Access to Mirror-Image Library of Natural Products*, Springer Theses,
https://doi.org/10.1007/978-981-10-6623-8_2

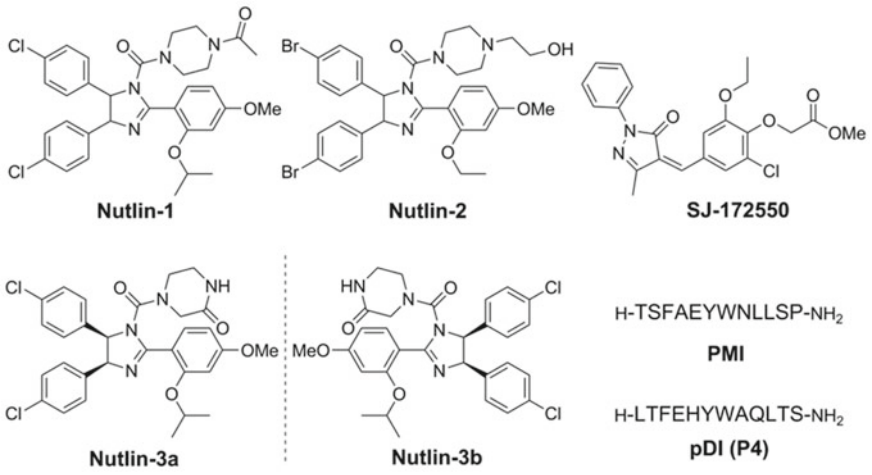


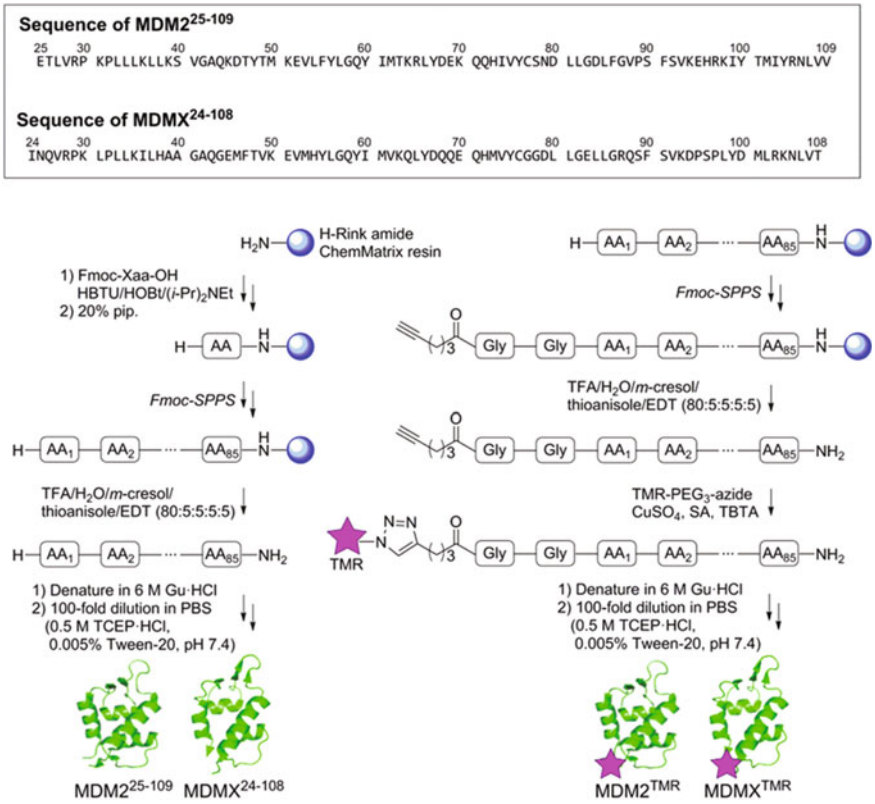
Fig. 2.1 Structures of MDM2–p53 and/or MDMX–p53 interaction inhibitors

[4]. As such, high expression of MDM2 and MDMX results in a reduction in the activity and expression level of the p53 in cancer cells, and PPI inhibitors against MDM2-p53 and/or MDMX-p53 interactions are expected as anticancer agents.

Inhibitory compounds that block the interaction between MDM2-p53 and MDMX-p53 have been identified using various types of screening technologies (Fig. 2.1) [5]. For example, MDM2-p53 interaction inhibitors, nutlin-1, -2, and -3, were identified by surface plasmon resonance (SPR) analysis [6]. SJ-172550 is an MDMX-p53 interaction inhibitor, which was identified by an FP assay [7]. p53-like peptide, PMI and pDI (also named P4), were identified as MDM2 and MDMX inhibitors by phage display [8]. These facile technologies are based on the evaluation of inhibitory effects by compounds against p53 binding to MDM2 and MDMX. Among the inhibitors, some chiral compounds have different activities between their enantiomers. For example, nutlin-3a potently binds to MDM2 (IC_{50}: 0.09 μM), while nutlin-3b (enantiomer of nutlin-3a) shows significantly less activity (IC_{50}: 13.6 μM). For identifying novel inhibitors from mirror-image natural products, strong enantiomeric recognitions of target proteins would be needed. Therefore, the author expected MDM2 and MDMX would have strong enantiomeric recognitions to small-molecules.

The author designed screening process using affinity-based chemical array screening and subsequent competitive FP assay to identify MDM2-p53 and MDMX-p53 interaction inhibitors efficiently. In this section, to investigate the feasibility of synthetic MDM2 and MDMX proteins for identification of their inhibitors, chemical synthesis of L-MDM2 and L-MDMX and application of the screening systems were performed.

Initially, the author investigated synthesis of MDM2 and MDMX and their fluorescent derivatives, which were used for chemical array screening. There have been a report on the synthesis of MDM2 and MDMX proteins by combining Boc-based



Scheme 2.1 Synthesis of MDM2 and MDMX proteins

SPPS with native chemical ligation [8]. Although this approach would be applicable to mid-sized protein synthesis, a more facile stepwise Fmoc-based SPPS approach was undertaken in this study (Scheme 2.1).

The p53-binding domain of MDM2 and MDMX (designated $MDM2^{25-109}$ and $MDMX^{24-108}$, respectively) were synthesized by standard Fmoc-based SPPS on an H-Rink Amide ChemMatrix resin using HBTU/HOBt/(*i*-Pr)$_2$NEt activation. After chain assembly, deprotection of the side chain protecting groups and cleavage from the resin with the cocktail [TFA/thioanisole/*m*-cresol/EDT/H_2O (80:5:5:5:5)], followed by RP-HPLC purification afforded the expected peptides. For the preparation of fluorescent MDM2 and MDMX proteins bearing a single tetramethylrhodamine moiety (designated $MDM2^{TMR}$ and $MDMX^{TMR}$, respectively), 5-hexynoic acid was conjugated via a diglycine linker on the resin. After purification of $MDM2^{25-109}$ and $MDMX^{24-108}$ with an N-terminal alkyne tag, treatment with TMR-$(PEG)_3$-azide in the presence of $CuSO_4$, sodium ascorbate (SA) and tris[(1-benzyl-1*H*-1,2,3-triazol-4-yl)methyl]amine (TBTA) provided fluorescent $MDM2^{TMR}$ and $MDMX^{TMR}$, respectively. The synthetic MDM2 and MDMX

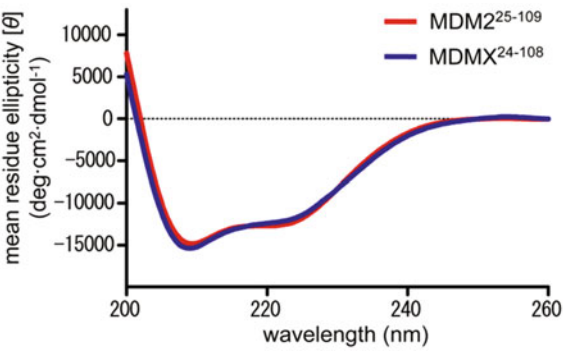


Fig. 2.2 CD spectra of $MDM2^{25-109}$ and $MDMX^{24-108}$. CD spectra of $MDM2^{25-109}$ and $MDMX^{24-108}$ were measured at room temperature in PBS containing 0.1 mM TCEP (pH 7.4)

proteins and their fluorescent derivatives, $MDM2^{TMR}$ and $MDMX^{TMR}$, were denatured in 6 M guanidine hydrochloride (Gu · HCl) solution and refolded by 100-fold dilution of the solution to PBS buffer (pH 7.4) containing 0.5 mM tris(2-carboxyethyl)phosphine (TCEP) and 0.005% Tween-20.

To validate the structures of the synthetic proteins, the author evaluated circular dichroism (CD) spectra of $MDM2^{25–109}$ and $MDMX^{24–108}$ (Fig. 2.2). Negative bands at 208 and 222 nm indicated the presence of α-helix secondary structure elements, which is characteristic for MDM2 and MDMX, and supported by previous crystal structure and CD analyses [9].

To further verify the biological activity of the synthetic proteins, binding affinities of MDM2 and MDMX towards the p53 peptide sequence were evaluated by SPR analysis. Varying concentrations of MDM2 and MDMX proteins were analyzed by a NeutrAvidin-coated NLC sensor chip (BioRad) on which the biotinylated wild-type p53 peptide (biotinyl-aminocaproyl-GSGSSQETFSDLWKLLPEN-NH_2) was immobilized (Fig. 2.3). $MDM2^{25–109}$ and $MDMX^{24–108}$ bound the p53 peptide with KD values of 0.803 and 2.22 μM, respectively, which supported the correct folding of these proteins [7]. The binding affinities (KD values) of $MDM2^{TMR}$ and $MDMX^{TMR}$ towards the p53 peptide were 0.616 and 2.14 μM, respectively, indicating that N-terminal modification of synthetic MDM2 and MDMX had no effect on the folding of these proteins or the biological functions [10].

The author next assessed the binding ability of $MDM2^{TMR}$ and $MDMX^{TMR}$ to the p53-like peptide (designated L-P4: H-LTFEHYWAQLTS-NH_2) immobilized on a microarray via carbene-mediated covalent bond formation. The enantiomer peptide (designated D-P4) was used as a negative control. $MDM2^{TMR}$ and $MDMX^{TMR}$ bound to L-p53 in a highly selective manner (Fig. 2.4). Higher MDM2–p53 binding compared with the MDMX–p53 interaction was observed, which is consistent with the more potent binding affinity of MDM2 to the p53 peptide in the SPR analysis.

To identify the inhibitor candidates for MDM2–p53 and MDMX–p53 interactions, the author next carried out chemical array screening using the $MDM2^{TMR}$ and $MDMX^{TMR}$ proteins (Fig. 2.5). Fifty-four hit compounds were identified from the 7600 compounds of the in-house chemical library that were immobilized on the

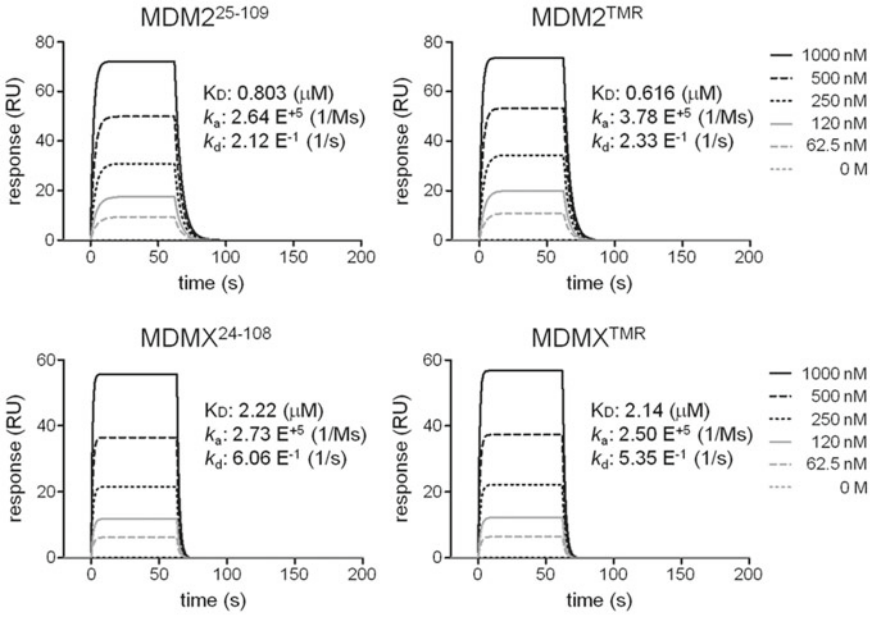


Fig. 2.3 SPR analysis of MDM2$^{25-109}$, MDM2^{TMR}, MDMX$^{24-108}$ and MDMX^{TMR} towards p53 peptide. KD values were determined by the calculation of k_a/k_d

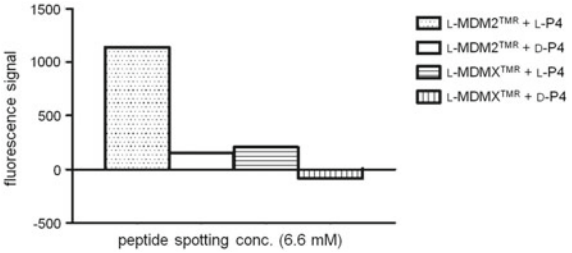


Fig. 2.4 Chemical array analysis of MDM2^{TMR} and MDMX^{TMR} proteins using both enantiomers of p53-like peptide (P4). MDM2^{TMR} and MDMX^{TMR} binding (1 μM in 1% skim-milk-TBS-T) were assessed using a chemical array, on which L-P4 (H-LTFEHYWAQLTS-NH_2) or D-P4 was spotted at the concentration of 6.6 mM

chemical array using 5 mM solutions. Of these, 6 compounds and 10 compounds showed selective binding to MDM2 and MDMX, respectively. The other 38 compounds exhibited binding to both MDM2 and MDMX.

To select small molecules that bind to the p53 binding pocket(s) in MDM2 and MDMX, the inhibitory effects on MDM2–p53 and MDMX–p53 interactions were further evaluated for the 54 hit compounds by a FP assay using a fluorescein-labeled P4 peptide (FAM-LTFEHYWAQLTS-NH_2) [11]. Three dual inhibitors against both interactions were obtained (Fig. 2.6): KPYA52218 (**1**), KPYB00497

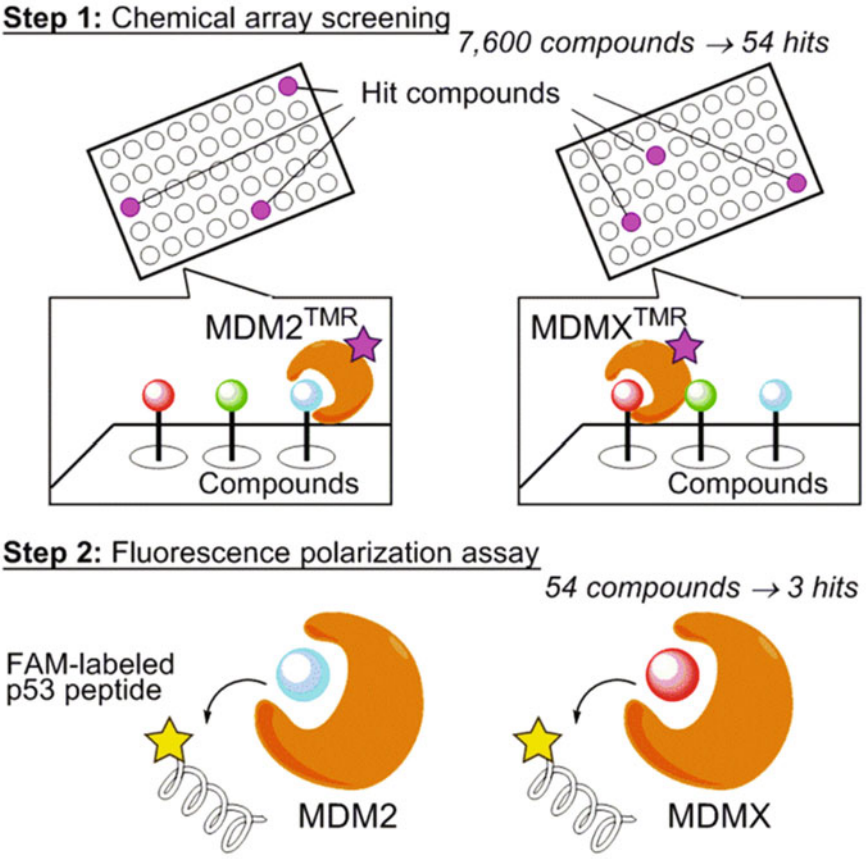


Fig. 2.5 Two-step screening process using $MDM2^{25-109}$ and $MDMX^{24-108}$ proteins

(**2**) and KPYB00556 (**3**) [IC_{50} (**1**) = 8.51 μM for MDM2, 32.4 μM for MDMX; IC_{50} (**2**) = 22.2 μM for MDM2, 42.1 μM for MDMX; IC_{50} (**3**) = 21.3 μM for MDM2, 52.5 μM for MDMX]. In the initial chemical array analysis, these compounds **1–3** were also identified to show dual binding to MDM2 and MDMX. Although MDM2 and MDMX share homologous sequences in their p53-binding domains, many of the known MDM2–p53 inhibitors do not effectively interact with MDMX–p53 probably because of the shallower and wider p53-binding pocket in MDMX [12]. Agents that disrupt MDM2-p53 interaction could inhibit tumor growth, but they are less effective in cancer cells that express high level of MDMX [13]. These dual inhibitors represent promising anticancer agent leads against cancer cells in which MDM2 and MDMX are overexpressed [14]. To gain insight into the effect on cell proliferation, growth inhibition by compounds **1–3** against human lung carcinoma-derived A549 cells was assessed. Compounds **1** and **3** showed no effect on cell growth, whereas cell growth was inhibited by compound **2** (EC_{50} = 13.7 μM).

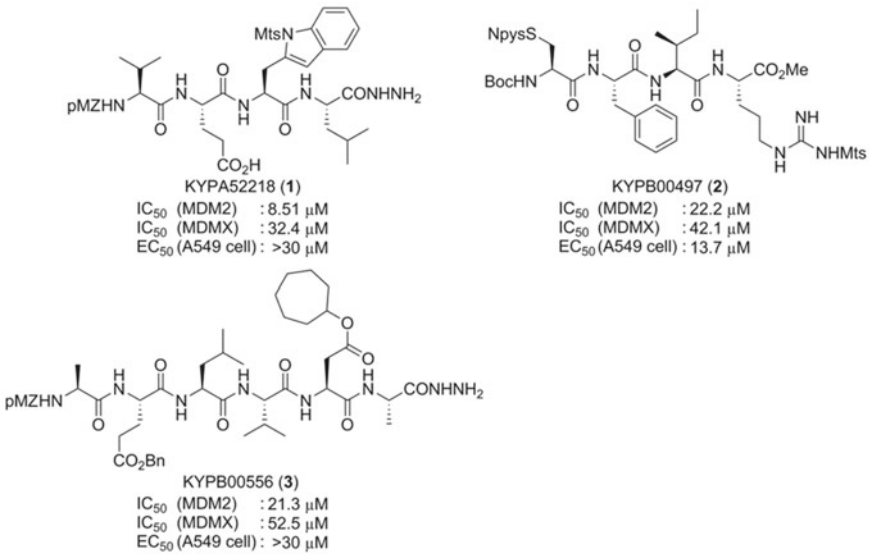


Fig. 2.6 Structures and biological activities of the hit compounds

Of note, in this screening process, the biological data from FP assays did not necessarily correspond to the binding ability obtained in the initial microarray screening, possibly owing to structural modification of the molecules bound to the microarray and potential binding to other binding site(s) than the p53 binging pocket. However, the microarray technology successfully facilitated the selection process for the identification of potential MDM2/MDMX-p53 interaction inhibitors.

In conclusion, the author has established screening protocols for binding molecules of MDM2 and MDMX by chemical array technology using synthetic fluorescent proteins. The preliminary screening of an in-house chemical library identified a number of peptidic binding molecules towards MDM2 and MDMX. The subsequent FP assay identified three dual inhibitors of MDM2–p53 and MDMX–p53 interactions. This new screening strategy for MDM2 and MDMX proteins using the affinity-based chemical array and subsequent FP assay should facilitate the identification process of MDM2–p53 and MDMX–p53 inhibitors.

2.1.1 Experimental Section

General Methods

Fmoc-protected amino acids were purchased from Watanabe Chemical Industries, Ltd. (Hiroshima, Japan), Kokusan Chemical Co. Ltd. (Kanagawa, Japan) or Sigma-Aldrich JAPAN (Tokyo, Japan). Other chemicals were purchased from Nacalai Tesque Inc. (Kyoto, Japan). For analytical HPLC for MDM2 and MDMX proteins,

Cosmosil 5C18-AR300 (4.6 × 250 mm, Nacalai Tesque Inc.) was employed with a linear gradient of CH_3CN containing 0.1% (v/v) TFA at a flow rate of 1 mL/min. Cosmosil 5C18-ARII column (4.6 × 250 mm, Nacalai Tesque Inc.) was employed for the analysis of the other peptides and peptidic compounds. ^{1}H NMR and ^{13}C NMR spectra were recorded using a JEOL ECA-500 spectrometer. ^{1}H NMR spectra were tabulated as follows: chemical shift, multiplicity (br: broad, s: singlet, d: doublet, t: triplet, q: quartet, m: multiplet), number of protons, and coupling constants.

Synthesis of MDM2$^{25–109}$ and MDMX$^{24–108}$

MDM2$^{25–109}$ and MDMX$^{24–108}$ were synthesized using automatic peptide synthesizer (PSSM-8, Shimadzu Corporation Ltd.) by Fmoc-based SPPS on H-Rink Amide ChemMatrix resin (0.4–0.6 mmol/g). For the side-chain protection, *t*-Bu ester for Asp and Glu; 2,2,4,6,7-pentamethyldihydrobenzofuran-5-sulfonyl (Pbf) for Arg; *t*-Bu for Thr, Tyr and Ser; Boc for Lys and Trp; and Trt for Gln, Asn, His, and Cys were employed for side-chain protection. Fmoc-Phe-OH (5 eq) was coupled by using HBTU (5 eq), HOBt (5 eq) and $(i\text{-Pr})_2$NEt (10 eq) in DMF-NMP, and the other Fmoc-protected amino acids were coupled by using HBTU (5 eq), HOBt (5 eq), $(i\text{-Pr})_2$NEt (10 eq) in DMF. In each coupling of amino acid, coupling reaction was carried out for 45 min twice. Fmoc-protecting group was removed by treating the resin with 20% piperidine in DMF. After chain assembly, the resulting protected peptide resin was treated with TFA/thioanisole/*m*-cresol/EDT/H_2O (80:5:5:5:5) at room temperature for 2 h. After removal of the resin by filtration, the filtrate was poured into ice-cold dry Et_2O. The resulting powder was collected by centrifugation and then washed three times with ice-cold dry Et_2O. The crude product was purified by HPLC on a Cosmosil 5C18-AR300 preparative column (Nacalai Tesque, 20 × 250 mm) with a linear gradient of CH_3CN containing 0.1% TFA at a flow rate of 8 mL/min, affording the expected peptides as white powder. The polypeptides were characterized by ESI-MS and purity was calculated as >95% by HPLC.

MS (ESI) for MDM2$^{25–109}$: Calcd for $C_{462}H_{739}N_{117}O_{123}S_4$: 10027.42; observed: $[M+12H]^{12+}$ *m/z* = 836.80, $[M+11H]^{11+}$ *m/z* = 912.45, $[M+10H]^{10+}$ *m/z* = 1003.91, $[M+9H]^{9+}$ *m/z* = 1115.26, $[M+8H]^{8+}$*m/z* = 1254.33, $[M+7H]^{7+}$ *m/z* = 1443.55, $[M+6H]^{6+}$ *m/z* = 1672.32.

MS (ESI) for MDMX$^{24–108}$: Calcd for $C_{438}H_{701}N_{117}O_{121}S_6$: 9733.08; observed: $[M+12H]^{12+}$ *m/z* = 811.68, $[M+11H]^{11+}$ *m/z* = 885.91, $[M+10H]^{10+}$ *m/z* = 974.42, $[M+9H]^{9+}$ *m/z* = 1082.62, $[M+8H]^{8+}$*m/z* = 1217.89, $[M+7H]^{7+}$ *m/z* = 1391.30, $[M+6H]^{6+}$ *m/z* = 1623.57.

Synthesis of MDM2^{TMR} and MDMX^{TMR}

Protected MDM2$^{25–109}$ and MDMX$^{24–108}$ were synthesized according to the identical procedure for the synthesis of MDM2$^{25–109}$ and MDMX$^{24–108}$. After assembling the full length sequence, two glycine residues (5 eq) and 5-hexynoic acid (5 eq) were coupled with HBTU (5 eq), HOBt (5 eq) and $(i\text{-Pr})_2$NEt (10 eq) in DMF. The resulting protected peptides were subjected to the deprotection, cleavage from resin, and HPLC purification. 200 mM $CuSO_4$ in H_2O (20 μL, 4 μmol) and 200 mM tris[(1-benzoyl-1*H*-1,2,3-triazol-4-yl)methyl]amine (TBTA) in DMSO (20 μL, 4 μmol) were added to H_2O-DMSO-*t*-BuOH (15:5:27, 470 μL) and the solution was stirred for 3 min.

Then, a sodium ascorbate solution (200 mM, 40 μL, 8 μmol) was added to the mixture in several pulses. This reagent cocktail was added to the mixture of MDM2 or MDMX (200 nmol) and TMR-$(PEG)_3$-azide (1 μmol) in DMSO (100 μL). After 15 min, the reaction mixture was purified by RP-HPLC on a Cosmosil 5C18-AR300 preparative column (Nacalai Tesque, 20 × 250 mm) with a linear gradient of CH_3CN containing 0.1% TFA at a flow rate of 8 mL/min. This purification afforded the TMR-labeled polypeptide dimer with a disulfide bond via the Cys residues (Cys^{82} in MDM2; Cys^{81} in MDMX). The collected TMR-labeled polypeptide dimer was dissolved in 10 mM TCEP · HCl in 6 M Gu · HCl/H_2O solution at 37 °C for 5 h, followed by RP-HPLC purification on a Cosmosil 5C18-AR300 preparative column (Nacalai Tesque, 20 × 250 mm) with a linear gradient of CH_3CN containing 0.1% TFA at a flow rate of 8 mL/min. This purification procedure afforded the monomer polypeptide as a pink powder (80 nmol, 40%).

MS (ESI) for $MDM2^{TMR}$: Calcd for $C_{505}H_{789}N_{125}O_{133}S_4$: 10865.79; observed: $[M+13H]^{13+}$ *m/z* = 836.55, $[M+12H]^{12+}$ *m/z* = 906.36, $[M+11H]^{11+}$ *m/z* = 989.10, $[M+10H]^{10+}$ *m/z* = 1087.60, $[M+9H]^{9+}$ *m/z* = 1208.20, $[M+8H]^{8+}$ *m/z* = 1359.00, $[M+7H]^{7+}$ *m/z* = 1553.07 $[M+6H]^{6+}$ *m/z* = 1812.23.

MS (ESI) for $MDMX^{TMR}$: Calcd for $C_{481}H_{751}N_{125}O_{131}S_6$: 10571.44; observed: $[M+14H]^{14+}$ *m/z* = 756.19, $[M+13H]^{13+}$ *m/z* = 814.28, $[M+12H]^{12+}$ *m/z* = 881.98, $[M+11H]^{11+}$ *m/z* = 962.15, $[M+10H]^{10+}$ *m/z* = 1058.36, $[M+9H]^{9+}$ *m/z* = 1175.58, $[M+8H]^{8+}$ *m/z* = 1322.82, $[M+7H]^{7+}$ *m/z* = 1511.24, $[M+6H]^{6+}$ *m/z* = 1762.70.

Folding of Synthetic MDM2 and MDMX Proteins

Lyophilized polypeptide (1 mg/mL) was dissolved in 6 M Gu · HCl containing 1 mM TCEP · HCl, followed by 100-fold dilution with PBS (pH 7.4) containing 0.5 mM TCEP · HCl and 0.005% Tween-20 at 4 °C. The solution was stored at 4 °C overnight, and the solution was concentrated using a MWCO 3000 centrifugal filtration membrane (Millipore, Amicon-Ultra 3 kDa).

Synthesis of p53 Peptides and Their Derivatives

All p53 and p53-like peptides were synthesized by Fmoc-based SPPS on Rink-amide resin (0.66 mmol/g, 45.5 mg, 0.025 mmol). Fmoc-protected amino acids (3 eq) were coupled by using DIPCI (3 eq) and HOBt (3 eq) in DMF. The Fmoc-protecting group was removed by treating the resin with 20% piperidine in DMF. Coupling of biotin (0.125 mmol) was carried out with HBTU (5 eq), HOBt (5 eq) and $(i\text{-Pr})_2NEt$ (10 eq) in DMF. Coupling of 5-carboxyfluorescein (5 eq) was carried out with DIPCI (5 eq) and HOBt (10 eq) in DMF. The resulting protected peptide resin was treated with TFA/thioanisole/*m*-cresol/EDT/H_2O (80:5:5:5:5) at room temperature for 2 h. After removal of the resin by filtration, the filtrate was poured into ice-cold dry Et_2O. The resulting powder was collected by centrifugation and then washed three times with ice-cold dry Et_2O. The crude product was purified by HPLC on a Cosmosil 5C18-ARII preparative column (Nacalai Tesque, 20 × 250 mm). All peptides were characterized by ESI-MS or MALDI-TOF-MS and the purity was ascertained by HPLC as >95%.

Biotin-labeled p53 peptide: MS (MALDI-TOF) calcd for $C_{108}H_{166}N_{27}O_{35}S$ $[M+H]^+$ 2434.18; found 2434.23.

L-P4: MS (MALDI-TOF) calcd for $C_{71}H_{100}N_{17}O_{19}$ $[M+H]^+$ 1494.74; found 1494.61.

D-P4: MS (MALDI-TOF) calcd for $C_{71}H_{100}N_{17}O_{19}$ $[M+H]^+$ 1494.74; found 1494.67.

Fluorescein-labeled P4 peptide: MS (ESI) calcd for $C_{92}H_{110}N_{17}O_{25}$ $[M+H]^+$ 1852.79, found 1852.95.

SPR Analysis

Binding kinetics analysis was carried out on a ProteOn XRP360 instrument using an N-terminal biotinylated wild-type p53 peptide immobilized on a NeutrAvidin-coated NLC sensor chip (43 RUs) at 20 °C. PBS (pH 7.4) containing 0.005% Tween-20 was used as the running buffer.

Screening by the Chemical Array

The photoaffinity linker-coated (PALC) slides were prepared according to previous reports using amine-coated slides and the photoaffinity linker [15]. A solution of compounds (5 mM in DMSO) from the in-house chemical library was immobilized onto the PALC glass slides with a chemical arrayer equipped with 24 stamping pins. The slides were exposed to UV irradiation of 4 J/cm^2 at 365 nm using a CL-1000L UV crosslinker (UVP, CA). The slides were washed successively with DMSO, DMF, acetonitrile, THF, dichloromethane, EtOH, and ultra-pure water (5 min, 3 times each), and dried. MDM2^{TMR} (1 μM in 1% skim-milk-TBS-T) and MDMX^{TMR} (1 μM in 1% skim-milk-TBS-T) were incubated with the glass slide for 1 h, and then washed with TBS-T (10 mM Tris-HCl, pH 8.0, 150 mM NaCl, 0.05% Tween-20) (5 min, 3 times). The slides were dried and scanned at 532 nm on a GenePix scanner. The fluorescence signals were quantified with GenePixPro.

Fluorescence Polarization Assay

Fluorescence polarization assays were carried out in PBS containing 0.005% Tween-20 using a fluorescein-labeled P4 peptide (0.5 nM) and MDM2$^{25–109}$ (10 nM) or MDMX$^{24–108}$ (50 nM) in black 96-well non-binding surface assay plates (Corning). For the inhibitor assays, compounds were preincubated with the synthetic protein for 30 min. The fluorescein-labeled P4 peptide was then added and incubated for 30 min. The unlabeled L-P4 peptide was used as the positive control. FP signals were analyzed using an EnVision Xcite plate reader with a 480-nm excitation filter and a 535-nm emission filter.

Cell Growth Inhibition Assay

A549 cells were cultured in DMEM medium (Sigma) supplemented with 10% (v/v) FBS at 37 °C in a 5% CO_2-incubator. Cell based assays using A549 cells were performed in 96-well plates (BD Falcon). A549 cells were seeded at 500 cells/well in 50 μL of DMEM, and placed for 6 h. Chemical compounds in DMSO were diluted 250-fold with the culture medium in advance. Following the addition of the fresh culture medium (40 μL), the chemical diluents (30 μL) were also added to the cell cultures. The final volume of DMSO in the medium was equal to 0.1% (v/v). The cells under chemical treatment were incubated for a further 72 h. The wells in the plates were washed twice with the cultured medium without phenol-red. After 1 h

incubation with 100 μL of the medium, the cell culture in each well was supplemented with the MTS reagent (20 μL, Promega), followed by incubation for an additional 40 min. Absorbance at 490 nm of each well was measured using a Wallac 1420 ARVO SX multilabel counter (Perkin Elmer).

Characterization Data of Hit Compounds (1–3)

KPYA 52218 (**1**). ^{1}H NMR (500 MHz, DMSO-d_6) δ 0.77 (t, J = 7.7 Hz, 6H), 0.85 (d, J = 6.3 Hz, 3H), 0.90 (d, J = 6.9 Hz, 3H), 1.45 (m, 1H), 1.56 (m, 1H), 1.64 (m, 1H), 1.74 (m, 1H), 1.87 (m, 1H), 1.95 (m, 1H), 2.21 (dd, J = 5.7, 10.3 Hz, 2H), 2.25 (s, 3H), 2.40 (s, 6H), 2.91 (dd, J = 10.3, 14.9 Hz, 1H), 3.10 (d, J = 6.0, 12.0 Hz, 1H), 3.73 (s, 3H), 3.88 (dd, J = 6.9, 8.6 Hz, 1H), 4.32 (m, 1H), 4.38 (m, 1H), 4.64 (m, 1H), 4.92 (q, J = 12.4 Hz, 2H), 6.88 (d, J = 8.6 Hz, 2H), 7.08 (s, 2H), 7.17–7.28 (m, 5H), 7.67 (s, 1H), 7.77 (dd, J = 2.3, 6.3 Hz, 1H), 7.82 (d, J = 8.0 Hz, 1H), 8.17 (d, J = 8.0 Hz, 1H), 8.42 (d, J = 8.0 Hz, 1H), 10.85 (br, 1H); ^{13}C NMR (500 MHz, DMSO-d_6) δ 17.9, 19.1, 20.4, 21.4, 21.9, 22.8, 24.0, 26.8, 29.7, 30.1, 40.6, 49.6, 51.3, 52.1, 55.0, 60.1, 65.3, 111.6, 113.7, 115.5, 120.0, 122.5, 124.3, 125.0, 128.7, 129.6, 129.8, 132.3, 133.8, 139.5, 144.2, 156.2, 158.9, 170.9, 171.3, 174.0; MS (MALDI-TOF) calcd for $C_{45}H_{59}N_7NaO_{11}S$ $[M+Na]^+$ 928.39, found 928.37.

KPYB 00497 (**2**). ^{1}H NMR (500 MHz, DMSO-d_6) δ 0.78 (t, J = 7.4 Hz, 3H), 0.82 (d, J = 6.9 Hz, 3H), 1.04 (m, 1H), 1.2–1.4 (m, 3H), 1.38 (s, 9H), 1.56 (m, 1H), 1.66 (m, 2H), 2.21 (s, 3H), 2.57 (s, 6H), 2.79 (dd, 1H), 2.9–3.1 (m, 5H), 3.59 (s, 3H), 4.1–4.2 (m, 3H), 4.59 (m, 1H), 6.47 (br, 1H), 6.91 (s, 2H), 7.1–7.2 (m, 5H), 7.24 (d, J = 8.0 Hz, 1H), 7.60 (dd, J = 4.6, 8.0 Hz, 1H), 7.87 (d, J = 8.0 Hz, 1H), 7.97 (d, J = 8.0 Hz, 1H), 8.35 (d, J = 8.0 Hz, 1H), 8.64 (dd, J = 1.1, 8.6 Hz, 1H), 8.89 (dd, J = 1.1, 4.6 Hz, 1H); ^{13}C NMR (500 MHz, DMSO-d_6) δ 10.8, 15.0, 20.3, 22.4, 24.1, 27.9, 28.1, 36.9, 37.4, 40.3, 51.7, 51.8, 53.2, 54.1, 56.3, 78.5, 122.0, 126.2, 127.8, 129.3, 131.0, 134.5, 136.9, 137.2, 139.6, 142.6, 154.1, 155.0, 155.1, 156.3, 170.0, 170.1, 171.0, 172.1; MS (MALDI-TOF) calcd for $C_{44}H_{61}N_9NaO_{11}S_3$ $[M+Na]^+$ 1010.35, found 1010.52.

KPYB 00556 (**3**). ^{1}H NMR (500 MHz, DMSO-d_6) δ 0.7–0.9 (m, 12H), 1.17 (d, J = 6.9 Hz, 3H), 1.21 (d, J = 7.4 Hz, 3H), 1.3–1.6 (m, 13H), 1.80 (m, 3H), 1.92 (m, 2H), 2.38 (m, 2H), 2.52 (dd, J = 1.78, 10.9 Hz, 1H), 2.75 (dd, J = 4.9, 16.3 Hz, 1H), 3.74 (s, 3H), 4.03 (m, 1H), 4.13 (dd, J = 6.9, 8.6 Hz, 1H), 4.23 (m, 1H), 4.30 (m, 1H), 4.35 (m, 1H), 4.60 (m, 1H), 4.80 (m, 1H), 4.92 (dd, J = 11.7, 30.6 Hz, 2H), 5.08 (s, 2H), 6.90 (d, J = 8.0 Hz, 2H), 7.27 (d, J = 8.6 Hz, 2H), 7.3–7.4 (m, 5H), 7.41 (d, J = 8.0 Hz, 1H), 7.77 (d, J = 8.0 Hz, 1H), 7.92 (d, J = 8.0 Hz, 1H), 7.96–7.98 (m, 2H), 8.24 (d, J = 8.0 Hz, 1H), 10.07 (br, 1H); ^{13}C NMR (500 MHz, DMSO-d_6) δ 17.9, 18.0, 19.0, 21.5, 22.3, 23.1, 24.0, 27.2, 27.7, 30.0, 30.7, 33.1, 36.0, 40.3, 47.1, 49.2, 50.1, 51.0, 51.5, 55.1, 57.4, 65.2, 65.4, 74.7, 113.7, 127.8, 127.9, 128.4, 128.8, 129.7, 136.2, 155.8, 159.0, 169.3, 169.9, 170.7, 170.8, 171.4, 171.7, 172.2, 172.5; MS (MALDI-TOF) calcd for $C_{49}H_{72}N_8NaO_{13}$ $[M+Na]^+$ 1003.51, found 1003.61.

2.2 Development of a Mirror-Image Screening Process by Using Synthetic Proteins

2.2.1 Screening of a Virtual Mirror-Image Library of Natural Products

Summary

The author established a novel screening approach for access to an unexplored mirror-image library of chiral natural product derivatives using D*-protein technology. Natural products and their derivatives are valuable resources for drug discovery. While most of chiral natural products are produced as single enantiomeric form in nature, mirror-image isomers of them are also potential resources for drug discovery because they have identical physicochemical properties and different biological properties. To screen the mirror-image library of chiral natural products, mirror-image screening strategy has been developed. Mirror-image MDM2 protein (named* D*-MDM2) was prepared by Fmoc-based solid phase peptide synthesis. By using* D*-MDM2 for screening, NP843, which was an α-tocopherol derivative, was ideintified as* D*-MDM2–*D*-p53 interaction inhibitors. The biological activities of ent-NP843 toward* L*-MDM2–*L*-p53 were also evaluated after preparing ent-NP843 by chiral pool synthesis. In this strategy, two chemical syntheses of mirror-image substances including a target protein and hit compound(s) allow the lead discovery from a virtual mirror-image library without synthesis of numerous mirror-image compounds.*

To screen the mirror-image library of chiral natural products and their derivatives for MDM2–p53 interaction inhibitors, the author performed the designed screening process using chemical array screening and subsequent FP assay with synthetic proteins [16]: (1) the D-protein of the target molecule is prepared by chemical protein synthesis; (2) using the synthetic D-protein, chiral natural products are screened to identify hit compound(s); (3) the mirror-image structure(s) of the hit compound(s) is synthesized; and (4) the biological activities for the native target molecule (L-protein) would be assessed (Fig. 2.7).

Initially, the author synthesized D-MDM2$^{25-109}$ by standard Fmoc-based solid-phase peptide synthesis (SPPS) according to the identical protocol described in Sect. 1 of Chap. 2. The tetramethylrhodamine (TMR)-labeled protein (D-MDM2^{TMR}) was also prepared by conjugation of TMR-$(PEG)_3$-azide onto the N-terminal alkyne tag of D-MDM2$^{25-109}$. The folded L-MDM2$^{25-109}$ and D-MDM2$^{25-109}$ had symmetric circular dichroism (CD) spectra, supporting the presence of mirror-image α-helices (Fig. 2.8).

To verify the biological activity of the synthetic MDM2 proteins, the binding affinities toward biotinylated p53 peptides (biotinyl-aminocaproyl-GSGSSQETFSDLWKLLPEN-NH_2) were evaluated by surface plasmon resonance (SPR) analysis (Fig. 2.9). The high-affinity bindings of L-MDM2–L-p53 peptide and D-MDM2–D-p53 peptide were observed [KD (L-MDM2–L-p53): 0.75 ± 0.04 μM; KD (D-MDM2–D-p53): 0.51 ± 0.02 μM], while the binding activities of

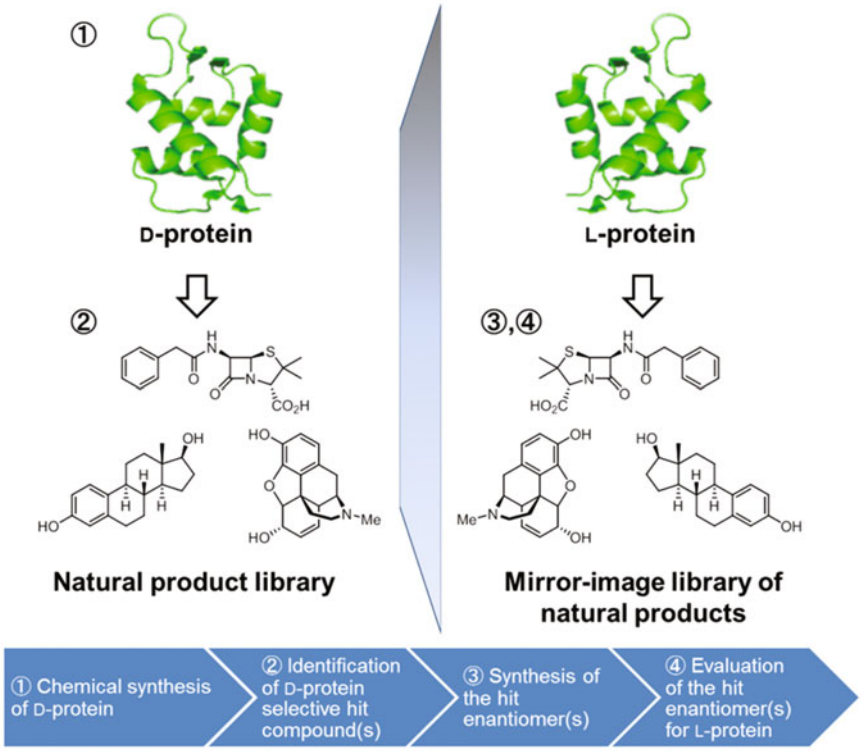


Fig. 2.7 Concept of mirror-image screening of chiral natural products

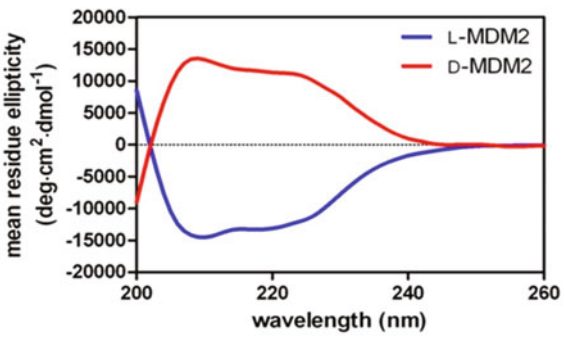
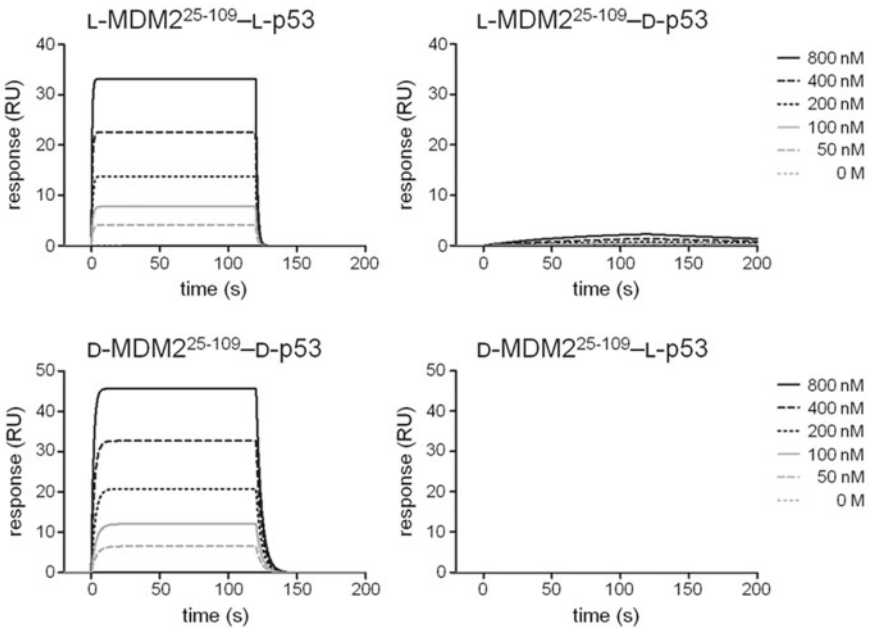


Fig. 2.8 CD spectra of synthetic L-MDM2 and D-MDM2 proteins. Spectra of L-MDM2$^{25–109}$ and D-MDM2$^{25–109}$ were measured at 25 °C in PBS containing 0.5 mM tris(2-carboxyethyl)phosphine (TCEP) and 0.005% Tween-20 (pH 7.4)

L-MDM2–D-p53 peptide and D-MDM2–L-p53 peptide were practically nil, suggesting high enantiomeric recognition of MDM2 toward p53.

The author next performed screening of natural products and their derivatives using both enantiomers of MDM2 protein. Chemical array screening of 22,293 compounds including natural products and their derivatives from RIKEN NPDepo



Analyte/Ligand	k_a (1/Ms)	k_d (1/s)	KD (mol/L)
L-MDM2$^{25-109}$/L-p53	$1.1 \pm 0.75\ E^{+6}$	$8.5 \pm 0.16\ E^{-1}$	$7.5 \pm 0.40\ E^{-7}$
D-MDM2$^{25-109}$/D-p53	$5.6 \pm 0.69\ E^{+5}$	$2.8 \pm 0.24\ E^{-1}$	$5.1 \pm 0.21\ E^{-7}$

Fig. 2.9 SPR analysis of p53 binding to synthetic MDM2$^{25–109}$. KD values were determined by the calculation of k_a/k_d

was carried out using L-MDM2^{TMR} and D-MDM2^{TMR}. Among 43 initial hit compounds, four compounds showed inhibitory activity against L-MDM2–L-p53 or D-MDM2–D-p53 interactions in the competitive binding inhibition assay by fluorescence polarization (FP) (Fig. 2.10). Of these, a chiral α-tocopherol derivative NP843 (**1a**) was identified to be a selective inhibitor against D-MDM2–D-p53 interaction (Fig. 2.11).

The next step was to verify the bioactivity of the enantiomeric form of **1a** (*ent*-NP843, **1b**) toward L-MDM2–L-p53 interaction. Compound **1b** was prepared by chiral pool synthesis from three commercially available optically pure components (Scheme 2.2). Initially, (*R*)-Roche ester-derived tosylate **2** was reacted with Grignard reagent **3**, prepared from (*S*)-citronellyl bromide, in the presence of copper catalyst. The subsequent deprotection of trityl-group gave alcohol **4**, after treatment with 1N NaOH for hydrolysis of the formyl ester derived from **4**. C1 elongation of **4** was then performed via tosylation and cyanation followed by reductions to give an alcohol **6**, which was converted into phosphonium salt **8**. (*R*)-Trolox-derived aldehyde **9** was employed as a chiral chromane component for Wittig reaction. The

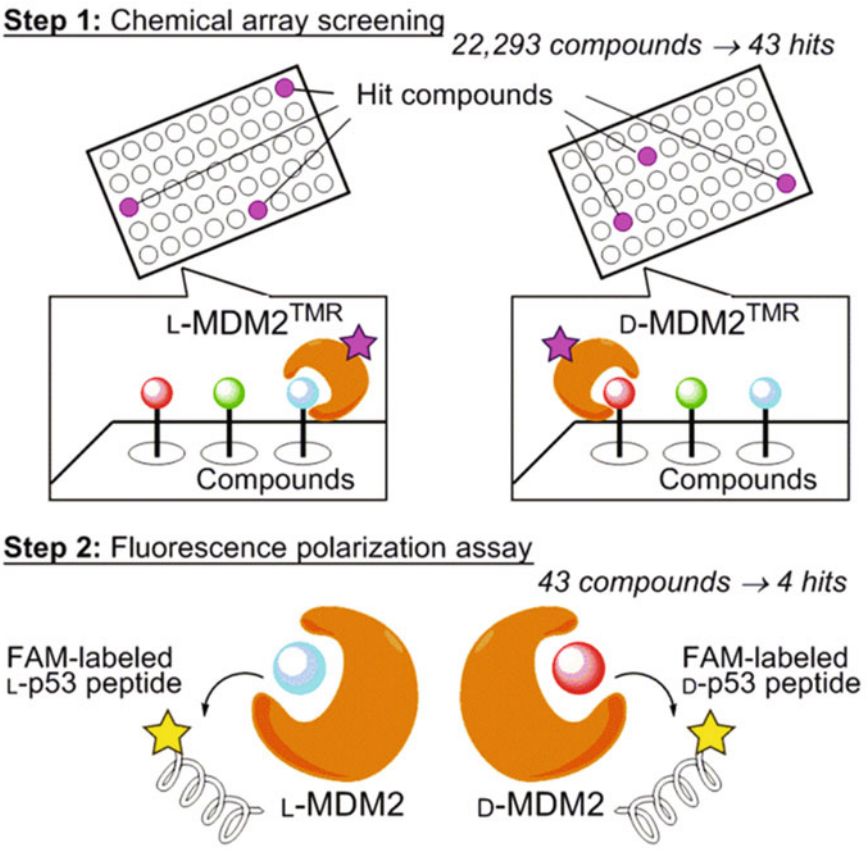


Fig. 2.10 Two-step screening process using D-MDM2$^{25-109}$

subsequent two-step catalytic reduction including PtO_2-mediated hydrogenation of olefins and subsequent Pd/C-mediated hydrogenolysis of the benzyl group provided the L-α-tocopherol (**10b**) in 84% yield. Alkylation of **10b** with bromide **11** followed by deprotection gave ketone **12b**. Construction of the left-part of the chromone substructure by treatment of **12b** with *N,N*-dimethylformamide dimethyl acetal (DMF-DMA) afforded **1b**.

The inhibitory activity of mirror-image compound **1b** against interaction between MDM2 and p53 peptide was evaluated by FP assay (Table 2.1). Compound **1b** inhibited L-MDM2–L-p53 interaction [IC_{50} (**1b**) = 7.6 ± 1.9 μM for L-MDM2–L-p53], while no inhibition was observed against D-MDM2–D-p53 interaction at 30 μM of **1b**. This corresponded with the inhibitory activities of the original hit **1a** against D-MDM2–D-p53 and L-MDM2–L-p53 interactions, respectively [IC_{50} (**1a**) = 6.5 ± 0.5 μM for D-MDM2–D-p53]. The similar inhibitory activities of **1b** were observed by SPR analysis and enzyme-linked immunosorbent assay (ELISA)

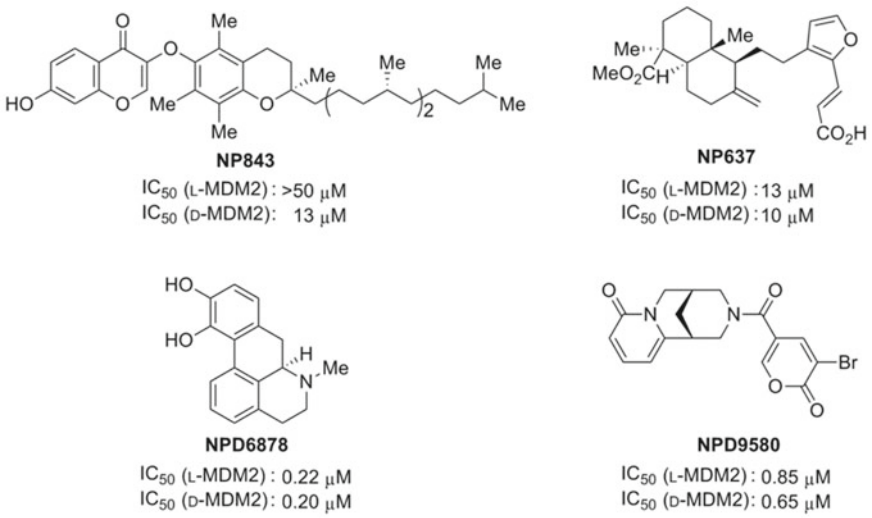


Fig. 2.11 Structures and biological activities of MDM2-p53 inhibitors from mirror-image screening. IC_{50} values were measured by FP assay using 0.5 nM FAM-labeled P4 peptide and 10 nM MDM2 protein

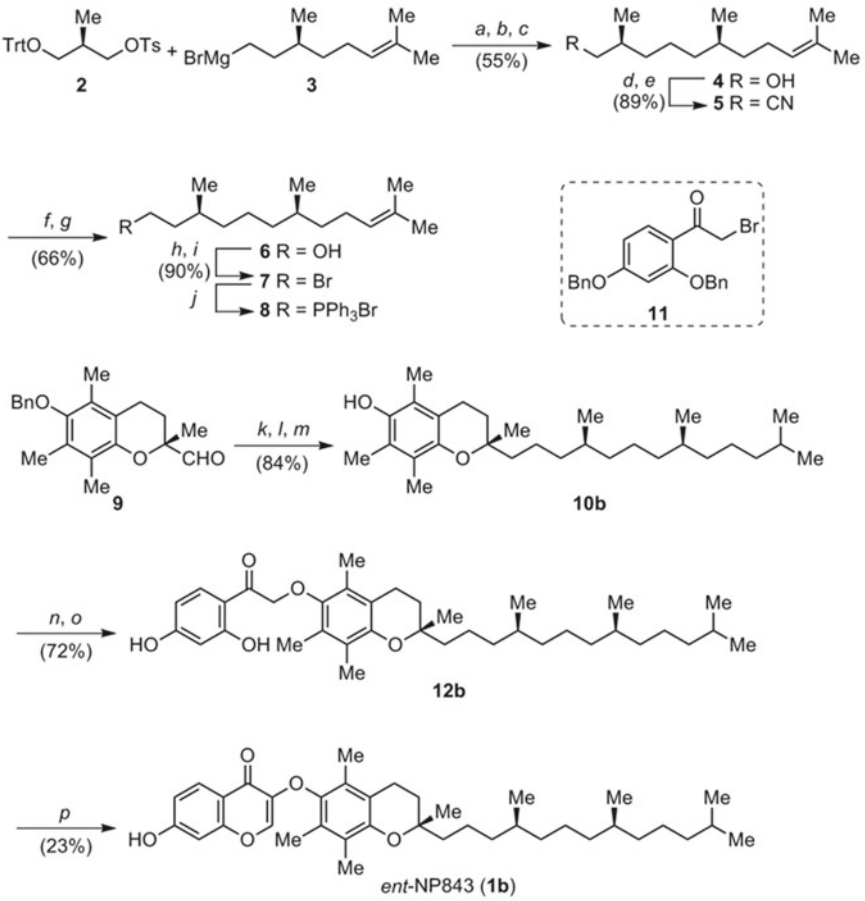
Table 2.1 Biological activities of NP843 and *ent*-NP843

Compounds	IC_{50} (μM)[a]		GI_{50} (μM)[b]	
	L-MDM2	D-MDM2	SJSA-1 cells	H1299 cells
Nutlin-3a	0.32 ± 0.03	>30	5.2 ± 0.19	>30
NP843 (**1a**)	>30	6.5 ± 0.5	>30	>30
ent-NP843 (**1b**)	7.6 ± 1.9	>30	>30	>30

[a]IC_{50} values for L/D-MDM2 were measured by FP assay using 1.0 nM fluorescein-labeled P4 peptide and 10 nM MDM2
[b]GI_{50} values for SJSA-1 and H1299 cells were measured by MTS assay

using synthetic and recombinant L-MDM2 proteins, respectively (Table 2.2). These data identified the mirror-image α-tocopherol derivative **1b** (*ent*-NP843) as a selective inhibitor of the L-MDM2–L-p53 interaction. Furthermore, the antiproliferative activity of *ent*-NP843 was investigated using cancer cells, SJSA-1 cells (MDM2 overexpressed) [17] and H1299 cells (no p53 expression) [18]. Unfortunately, no antiproliferative activities of *ent*-NP843 against SJSA-1 and H1299 cells were observed at 30 μM (Table 2.1).

Further structure–activity study of compound **1b** and the derivatives revealed the structural requirements for inhibition of L-MDM2–L-p53 interaction (Table 2.3). The author designed two diastereomers of compound **1b**: epimer **1c** at the tetrasubstituted carbon on the chromane scaffold, and diastereomer **1d** with two epimeric methyl groups on the right-hand alkyl chain (mirror-image of **1c**) (Fig. 2.12). Com-



Scheme 2.2 Synthetic scheme for *ent*-NP843. *Reagents and condition*: *a* Li_2CuCl_4, THF, 0 °C; *b* HCO_2H, Et_2O, rt; *c* NaOH, MeOH/H_2O, rt; *d* TsCl, pyridine, 0 °C; *e* NaCN, DMSO, rt; *f* DIBAL-H, THF/CH_2Cl_2, −78 °C, then H_3O^+; *g* DIBAL-H, THF/CH_2Cl_2, −78 °C; *h* TsCl, pyridine, 0 °C; *i* LiBr, acetone, reflux; *j* PPh_3, neat, 100 °C; *k* LHMDS, **8**, THF, −40 °C to rt; *l* H_2, PtO_2, TBME, rt; *m* H_2, Pd/C, MeOH, rt; *n* **11**, K_2CO_3, DMF, rt; *o* H_2, Pd/C, EtOAc, rt; *p* DMF-DMA, THF, reflux

pound **1d**, having a tetrasubstituted carbon with (*S*)-configuration on the chromane skeleton (identical to that of compound **1b**) reproduced the bioactivity of **1b** against L-MDM2–L-p53 interaction [IC_{50} (**1d**) = 6.9 ± 1.9 μM for L-MDM2–L-p53], while compound **1c** with (*R*)-configuration (identical to that of compound **1a**) showed no inhibition. However, for D-MDM2–D-p53 inhibition, compound **1c** was potent [IC_{50} (**1c**) = 7.8 ± 2.0 μM for D-MDM2–D-p53]. These results indicate that the stereochemistry of the tetrasubstituted carbon on the chromane skeleton is dominant in the chiral recognition by L-MDM2 protein when compared with the stereocenters on the extended alkyl chain. To demonstrate the significance of the aliphatic chain length

Table 2.2 Inhibitory Activities of NP843 and *ent*-NP843 by SPR Analysis and ELISA

Compound	IC_{50} (μM)[a]	
	SPR	ELISA
L-P4	0.011 ± 0.001	0.066 ± 0.007
D-P4	>1.0	>1.0
NP843 (**1a**)	>30	>30
ent-NP843 (**1b**)	3.1 ± 0.5	16.7 ± 1.1

[a]IC_{50} values were evaluated in triclicate assays

Table 2.3 Biological activity of NP843 derivatives

Compounds	IC_{50} (μM)[a]	
	L-MDM2	D-MDM2
1c	>30	7.8 ± 2.0
1d	6.9 ± 1.9	>30
13a	>30	>30
13b	>30	>30
14a	>30	>30
14b	>30	>30

[a]IC_{50} values for L/D-MDM2 were measured by FP assay using 1.0 nM fluorescein-labeled P4 peptide and 10 nM MDM2

of **1b**, the author also designed derivatives **13a**,**b** and **14a**,**b** with shorter isoprene units (Fig. 2.12). Derivatives **13a**,**b** and **14a**,**b** showed no inhibitory activity against L-MDM2–L-p53 interaction (nor against D-MDM2–D-p53 interaction). These results suggest a chain length of three isoprene units is indispensable for biological activity of compound **1b**.

In this study, isolated natural products and derivatives, which were immobilized on microarray slides, were used as a screening resource. This approach would be further applicable to the mirror-image screening of mixture samples from natural resources including crude plant extracts and fermentation broth extracts, which could provide unprecedented opportunity to explore diastereomeric interactions between the mirror-image structures of chiral ingredients and native proteins. Once the hit extract(s) is identified, structural determination of the active ingredient(s) and synthesis of its enantiomer(s) would be needed. In this way, novel hit compound(s) with "unnatural" chirality would be obtained with a high probability. It is the expectation that future analysis of screening data sets against a number of target molecules may give some insights into the value of mirror-image natural resources for drug discovery.

In this strategy, two chemical syntheses of mirror-image substances (target protein and initial hit compound), and chemical array technology using synthetic D-protein facilitated access to a variety of virtual mirror-image natural products. For further applications to other molecular targets, rapid and efficient preparations of mirror-

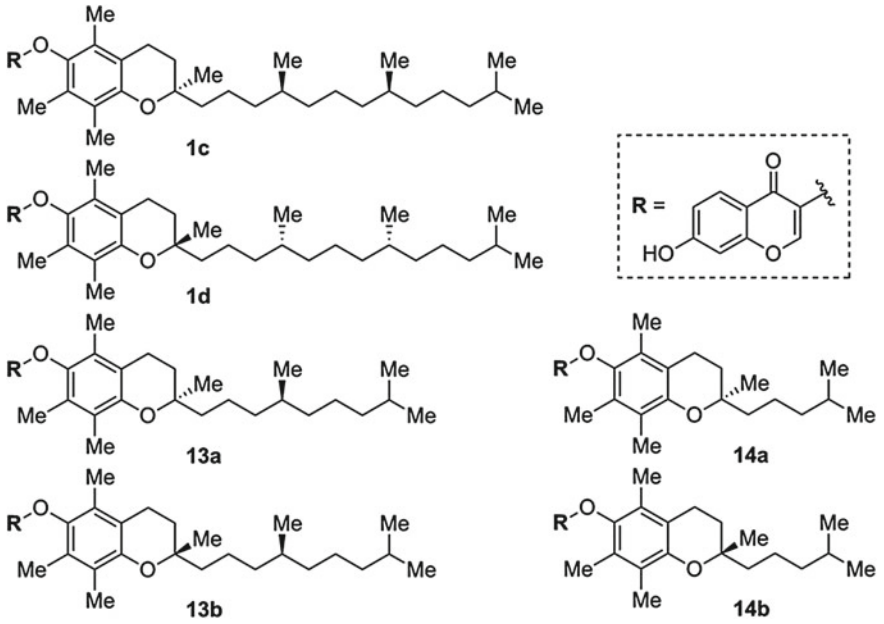


Fig. 2.12 Structures of NP843 derivatives

image biomolecules and natural product hit(s) are essential because these cannot be generated via protein expressions or conventional cultivations. Recent progress in chemical protein synthesis has increased the availability of synthetic proteins, even with highly functional modification(s) [19]. Although this study demonstrates mirror-image screening for protein–protein interaction inhibitors, the targets could be extended to enzyme inhibitors and receptor ligands once the counterpart mirror-image biomolecule(s) are available [20]. A number of recent advances in efficient synthetic strategies to access unique and complex frameworks in natural products should also contribute to the concise preparation of mirror-image structure(s) of natural product hit compounds. Thus, investigation of the bioactivities and functions of virtual mirror-image compounds is achievable only by using advanced synthetic organic chemistry technologies.

In summary, the author has established a novel screening process for a virtual mirror-image library of chiral natural products and derivatives. Chemically synthesized mirror-image MDM2 was applied for chemical array screening of a library of natural product derivatives, identifying novel tocopherol derivative NP843 (**1a**) as a D-MDM2–D-p53 interaction inhibitor. Chemical synthesis of the enantiomeric compound (**1b**) enabled the validation of the inhibitory activity of **1b** against L-MDM2–L-p53 interaction. The selective recognition by MDM2 was attributed to the stereochemistry of the tetrasubstituted carbon on the chromane skeleton of **1b**. The aliphatic side chain of three isoprene units was also needed for inhibition. In contrast to conventional screenings, this process could identify hit compounds from

unavailable mirror-image chiral natural products, thus providing unprecedented lead compounds for drug discovery. This is the first application of mirror-image protein technology to the screening of chiral small molecules including natural products.

2.2.2 *Experimental Section*

General Methods

^{1}H NMR and ^{13}C NMR spectra were recorded using a JEOL ECA-500 spectrometer. Chemical shifts are reported in δ (ppm) relative to Me_4Si (in $CDCl_3$). ^{13}C NMR spectra were referenced to the residual $CHCl_3$ (in $CDCl_3$). ^{1}H NMR spectra were tabulated as follows: chemical shift, multiplicity (br: broad, s: singlet, d: doublet, t: triplet, q: quartet, m: multiplet), number of protons, and coupling constants. Exact mass (HRMS) spectra were recorded on a JMS-HX/HX 110A mass spectrometer or Shimadzu LC-ESI-IT-TOF-MS equipment. Melting points were measured by a hot stage melting point apparatus (uncorrected). For flash chromatography, Wakogel C-300E (Wako) was employed. For analytical HPLC for MDM2 proteins, Cosmosil 5C18-AR300 (4.6 × 250 mm, Nacalai Tesque Inc.) was employed with a linear gradient of CH_3CN containing 0.1% (v/v) TFA aq. at a flow rate of 1 mL/min. Cosmosil 5C18-ARII column (4.6 × 250 mm, Nacalai Tesque Inc.) was employed for the analysis of the other peptides. The purity of all compounds for biological evaluations was determined by combustion analysis (>95%).

Synthesis of MDM2$^{25–109}$ and MDM2^{TMR} Proteins

L-MDM2$^{25–109}$, L-MDM2^{TMR}, D-MDM2$^{25–109}$ and D-MDM2^{TMR} proteins were synthesized by the identical protocol in Sect. 1 of Chap. 2. Briefly, protected MDM2$^{25–109}$ was synthesized by a standard protocol of Fmoc-based SPPS using automatic peptide synthesizer (PSSM-8, Shimadzu Corporation Ltd.) on H-Rink Amide ChemMatrix resin (0.4–0.6 mmol/g) using HBTU/HOBt/(i-Pr)$_2$NEt activation. The resulting protected peptide resin was treated with TFA/thioanisole/m-cresol/EDT/H_2O (80:5:5:5:5) at room temperature for 2 h. After removal of the resin by filtration, the filtrate was poured into ice-cold dry Et_2O. The resulting powder was collected by centrifugation and then washed with ice-cold dry Et_2O three times. The crude product was purified by HPLC to provide MDM2$^{25–109}$ proteins as white powder (Fig. 2.13).

For the synthesis of MDM2^{TMR} proteins, two glycines and 5-hexynoic acid were coupled with HBTU/HOBt/(i-Pr)$_2$NEt. The resulting protected peptides were treated with the deprotection cocktail as above to provide alkyne-conjugated proteins. Subsequently, treatment of the proteins with TMR-(PEG)$_3$-azide in the presence of Cu(I) provided TMR-labeled MDM2^{TMR} proteins as pink powder (Fig. 2.13).

ESI-MS for L-MDM2$^{25–109}$: Calcd for $C_{462}H_{739}N_{117}O_{123}S_4$: 10027.42; observed: $[M+12H]^{12+}$ m/z = 836.74, $[M+11H]^{11+}$ m/z = 912.76, $[M+10H]^{10+}$ m/z = 1003.86, $[M+9H]^{9+}$ m/z = 1115.39, $[M+8H]^{8+}$ m/z = 1254.76, $[M+7H]^{7+}$ m/z = 1434.00.[1]

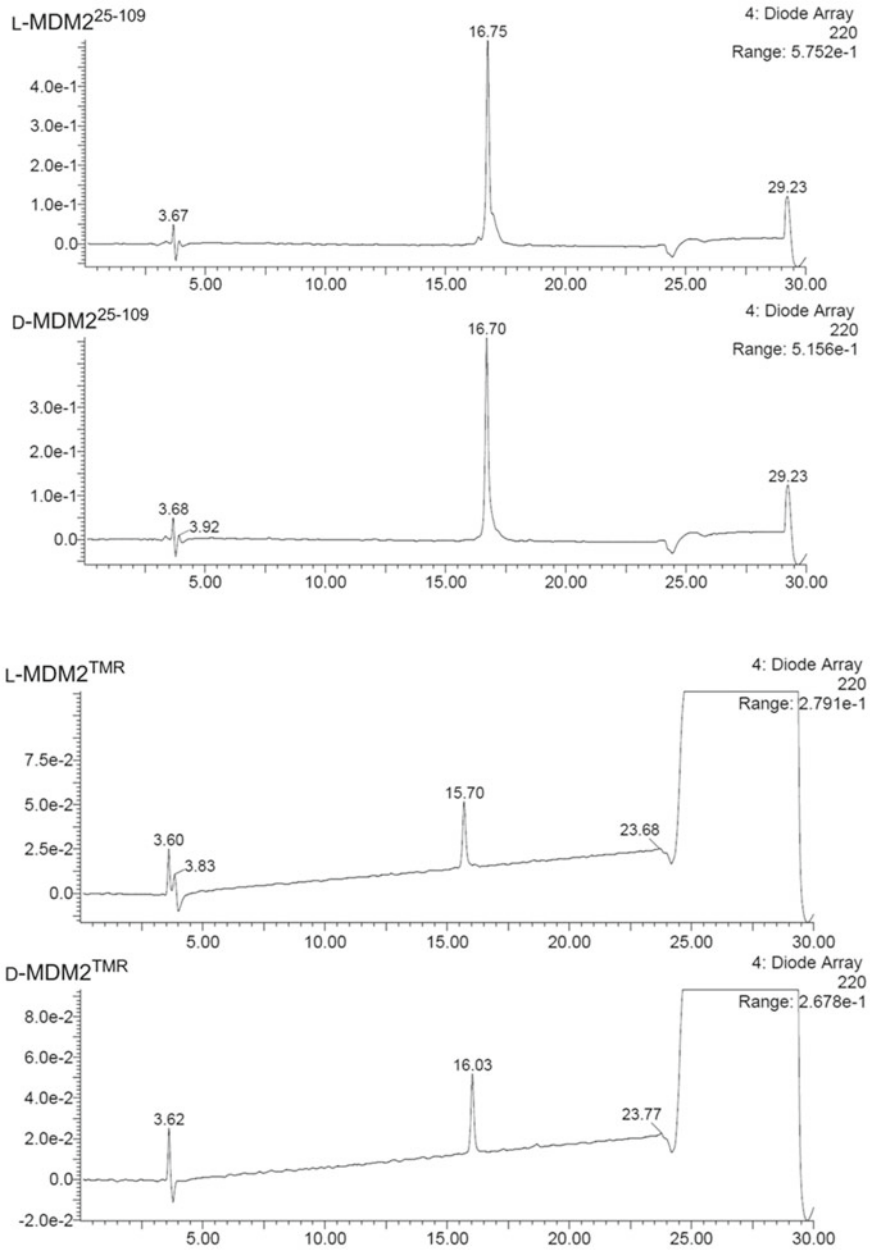


Fig. 2.13 LC–MS chromatograms of purified synthetic MDM2$^{25-109}$ and MDM2^{TMR} proteins. *HPLC conditions*: HPLC analysis was performed at 25 °C on a Cosmosil 5C18-AR300 preparative column (Nacalai Tesque, 4.5 × 250 mm) with a linear gradient of 30–50% CH_3CN containing 0.1% TFA at a flow rate of 1 mL/min over 20 min

ESI-MS for D-MDM2$^{25–109}$: Calcd for $C_{462}H_{739}N_{117}O_{123}S_4$: 10027.42; observed: $[M+12H]^{12+}$ m/z = 836.68, $[M+11H]^{11+}$ m/z = 912.77, $[M+10H]^{10+}$ m/z = 1003.94, $[M+9H]^{9+}$ m/z = 1115.46, $[M+8H]^{8+}$ m/z = 1254.85, $[M+7H]^{7+}$ m/z = 1433.42.

ESI-MS for L-MDM2^{TMR}: Calcd for $C_{505}H_{789}N_{125}O_{133}S_4$: 10865.79; observed: $[M+13H]^{13+}$ m/z = 836.94, $[M+12H]^{12+}$ m/z = 906.78, $[M+11H]^{11+}$ m/z = 989.03, $[M+10H]^{10+}$ m/z = 1087.90, $[M+9H]^{9+}$ m/z = 1208.38, $[M+8H]^{8+}$ m/z = 1359.59.[1]

ESI-MS for D-MDM2^{TMR}: Calcd for $C_{505}H_{789}N_{125}O_{133}S_4$: 10865.79; observed: $[M+13H]^{13+}$ m/z = 836.65, $[M+12H]^{12+}$ m/z = 906.65, $[M+11H]^{11+}$ m/z = 989.11, $[M+10H]^{10+}$ m/z = 1088.17, $[M+9H]^{9+}$ m/z = 1208.45, $[M+8H]^{8+}$ m/z = 1359.80.

Folding of Synthetic MDM2$^{25–109}$ and MDM2^{TMR} Proteins

Folding of synthetic MDM2 proteins were carried out by the identical protocol in Sect. 1 of Chap. 2 [16]. Lyophilized polypeptide was dissolved in 6 M guanidine hydrochloride (Gu · HCl) (1 mg/mL) followed by 100-fold dilution with PBS (pH 7.4) containing 0.5 mM TCEP · HCl and 0.005% Tween-20 at 4 °C. The solution was stored at 4 °C overnight, and the solution was concentrated using a MWCO 3000 centrifugal filtration membrane (Millipore, Amicon-Ultra 3 kDa) (3 times).

Synthesis of p53 Peptides and Their Derivatives

p53 peptides were synthesized by Fmoc-based SPPS on Rink-amide resin (0.66 mmol/g, 45.5 mg, 0.025 mmol) according to the identical protocol in the previous report [16]. Fmoc-protected amino acids (3 eq) were coupled by using DIPCI (3 eq) and HOBt (3 eq) in DMF. The Fmoc-protecting group was removed by treatment of the resin with 20% piperidine in DMF. Coupling of biotin (0.125 mmol) was carried out with HBTU (5 eq), HOBt (5 eq) and $(i\text{-Pr})_2$NEt (10 eq) in DMF. Coupling of 5-carboxyfluorescein (5 eq) was carried out with DIPCI (5 eq) and HOBt (10 eq) in DMF. The resulting protected peptide resin was treated with TFA/thioanisole/*m*-cresol/EDT/H_2O (80:5:5:5:5) at room temperature for 2 h. After removal of the resin by filtration, the filtrate was poured into ice-cold dry Et_2O. The resulting powder was collected by centrifugation and then washed with ice-cold dry Et_2O three times. The crude product was purified by HPLC on a Cosmosil 5C18-ARII preparative column (Nacalai Tesque, 20 × 250 mm). All peptides were characterized by MALDI-TOF-MS.

Biotin-labeled L-p53 peptide (biotinyl-aminocaproyl-GSGSSQETFSDLWKLLPEN-NH_2): MS (MALDI-TOF) calcd for $C_{108}H_{166}N_{27}O_{35}S$ $[M+H]^+$ 2434.19; found: 2434.13.

Biotin-labeled D-p53 peptide: MS (MALDI-TOF) calcd for $C_{108}H_{166}N_{27}O_{35}S$ $[M+H]^+$ 2434.19; found: 2434.12.

L-P4 (H-LTFEHYWAQLTS-NH_2): MS (MALDI-TOF) calcd for $C_{71}H_{100}N_{17}O_{19}$ $[M+H]^+$ 1494.74; found: 1494.75.

D-P4: MS (MALDI-TOF) calcd for $C_{71}H_{100}N_{17}O_{19}$ $[M+H]^+$ 1494.74; found: 1494.73.

5-Carboxyfluorescein-labeled L-P4 (5-FAM-LTFEHYWAQLTS-NH_2): MS (MALDI-TOF) calcd for $C_{92}H_{110}N_{17}O_{25}$ $[M+H]^+$ 1852.79; found: 1852.80.

5-Carboxyfluorescein-labeled D-P4: MS (MALDI-TOF) calcd for $C_{92}H_{110}N_{17}O_{25}$ $[M+H]^+$ 1852.79; found: 1852.76.

(2*S*,6*R*)-2,6,10-Trimethylundec-9-en-1-ol (4)
To a stirred mixture of Mg (1.00 g, 41.2 mmol) in THF (6.6 mL) was added dropwise (*S*)-citronellyl bromide (6.00 g, 27.4 mmol) in THF (16.8 mL) over 2 h using syringe pump at 60 °C to give Grignard reagent **3**. To a stirred solution of **2** [21] (6.9 g, 14.2 mmol) in THF (31.0 mL) were added the reagent **3** and 0.1 M Li_2CuCl_4 in THF (27.0 mL, 2.70 mmol) at −40 °C. The resulting mixture was stirred at −40 °C overnight and the reaction was quenched with saturated NH_4Cl at 0 °C. The whole was extracted with Et_2O and the extract was washed with H_2O and brine, and dried over $MgSO_4$. The filtrate was concentrated under reduced pressure. The oily residue was dissolved in hexane and the solution was filtrated through a short pad of silica gel and the filtrate was concentrated under reduced pressure. To a stirred solution of the residue in dry Et_2O (120 mL) was added HCO_2H (120 mL) dropwise at 0 °C under argon, and the stirring was continued for 1 h. After toluene (150 mL) was added, the solution was concentrated under reduced pressure. 1N NaOH in MeOH/H_2O (1:1, 100 mL) was added to the residue and the mixture was stirred for 10 min. The mixture was concentrated under reduced pressure. The residue was extracted with Et_2O and the extract was dried over $MgSO_4$. The filtrate was concentrated under reduced pressure, and the residue was purified by column chromatography to give the title compound **4** as a colorless oil (1.67 g, 55%). $[\alpha]_D^{25}$ −7.5 (*c* 1.10, $CHCl_3$); IR (neat): 3319 (OH), 1035 (C–O); ^{1}H NMR (500 MHz, $CDCl_3$) δ 0.86 (d, J = 6.3 Hz, 3H), 0.93 (d, J = 6.3 Hz, 3H), 1.04–1.42 (m, 9H), 1.60 (s, 3H), 1.58–1.65 (m, 1H), 1.68 (s, 3H), 1.89–2.03 (m, 2H), 3.42 (dd, J = 10.3, 6.3 Hz, 1H), 3.51 (dd, J = 10.6, 6.0 Hz, 1H), 5.09–5.11 (m, 1H); ^{13}C NMR (125 MHz, $CDCl_3$) δ 16.6, 17.6, 19.6, 24.3, 25.5, 25.7, 32.4, 33.4, 35.8, 37.1, 37.2, 68.4, 125.0, 131.0. HRMS (FAB) calcd for $C_{14}H_{29}O$ (MH^+): 213.2213; found: 213.2217.

(2*R*,6*S*)-2,6,10-Trimethylundec-9-en-1-ol (*ent*-4)
According to the procedure described for the preparation of **4**, compound *ent*-**2** (5.00 g, 10.3 mmol) was converted into *ent*-**4** with (*R*)-citronellyl bromide (6.40 g, 29.2 mmol) as a colorless oil (996 mg, 46%). $[\alpha]_D^{25}$ +7.4 (*c* 1.17, $CHCl_3$); IR (neat): 3357 (OH), 1034 (C-O); ^{1}H NMR (500 MHz, $CDCl_3$) δ 0.86 (d, J = 6.9 Hz, 3H), 0.92 (d, J = 6.3 Hz, 3H), 1.03–1.41 (m, 9H), 1.60 (s, 3H), 1.58–1.65 (m, 1H), 1.68 (s, 3H), 1.89–2.03 (m, 2H), 3.42 (dd, J = 10.3, 6.3 Hz, 1H), 3.51 (dd, J = 10.6, 6.3 Hz, 1H), 5.09–5.11 (m, 1H); ^{13}C NMR (125 MHz, $CDCl_3$) δ 16.6, 17.6, 19.6, 24.3, 25.5, 25.7, 32.4, 33.4, 35.8, 37.1, 37.2, 68.4, 125.0, 131.0. HRMS (FAB) calcd for $C_{14}H_{29}O$ (MH^+): 213.2213; found: 213.2223.

(3*S*,7*R*)-3,7,11-Trimethyldodec-10-enenitrile (5)
To a stirred solution of compound **4** (1.26 g, 5.93 mmol) in pyridine (4.3 mL) was added TsCl (1.40 g, 7.72 mmol) at 0 °C. After the mixture was stirred for 2 h, saturated aqueous solution of citric acid was added. The whole was extracted with Et_2O and the extract was washed with H_2O and brine, and dried over $MgSO_4$. The extract was concentrated under reduced pressure after filtration through a short pad of silica gel to give a crude sulfonate. To a stirred solution of the sulfonate in DMSO (13.0 mL) was added NaCN (0.581 g, 11.86 mmol) at room temperature. After the

mixture was stirred overnight, saturated aqueous solution of NH_4Cl was added. The whole was extracted with $CHCl_3$ and the extract was washed with H_2O and brine, and dried over $MgSO_4$. The filtrate was concentrated under reduced pressure, and the residue was purified by column chromatography to give the title cyanide **5** as a colorless oil (1.17 g, 89%). $[\alpha]_D^{25}$ +5.2 (*c* 1.02, $CHCl_3$); IR (neat): 2247 (C≡N); ^{1}H NMR (500 MHz, $CDCl_3$) δ 0.87 (d, *J* = 6.3 Hz, 3H), 1.07 (d, *J* = 6.9 Hz, 3H), 1.07–1.17 (m, 2H), 1.23–1.43 (m, 7H), 1.60 (s, 3H), 1.69 (s, 3H), 1.81–1.89 (m, 1H), 1.89–2.03 (m, 2H), 2.23 (dd, *J* = 16.6, 6.9 Hz, 1H), 2.32 (dd, *J* = 16.6, 5.7 Hz, 1H), 5.09–5.11 (m, 1H); ^{13}C NMR (125 MHz, $CDCl_3$) δ 17.6, 19.5 (2C), 24.2, 24.4, 25.5, 25.7, 30.5, 32.3, 36.2, 36.8, 37.0, 119.0, 124.9, 131.1. HRMS (FAB) calcd for $C_{15}H_{28}N$ (MH^+): 222.2216; found: 222.2224.

(3*R*,7*S*)-3,7,11-Trimethyldodec-10-enenitrile (*ent*-5)
According to the procedure described for the preparation of **5**, compound *ent*-**4** (950 mg, 4.47 mmol) was converted into *ent*-**5** as a colorless oil (948 mg, 96%). $[\alpha]_D^{25}$ −5.3 (*c* 1.08, $CHCl_3$); IR (neat): 2247 (C≡N); ^{1}H NMR (500 MHz, $CDCl_3$) δ 0.87 (d, *J* = 6.3 Hz, 3H), 1.07 (d, *J* = 6.9 Hz, 3H), 1.09-1.17 (m, 2H), 1.21–1.43 (m, 7H), 1.61 (s, 3H), 1.69 (s, 3H), 1.81–1.89 (m, 1H), 1.89–2.03 (m, 2H), 2.24 (dd, *J* = 16.6, 6.9 Hz, 1H), 2.32 (dd, *J* = 16.6, 5.7 Hz, 1H), 5.08–5.11 (m, 1H); ^{13}C NMR (125 MHz, $CDCl_3$) δ 17.6, 19.5 (2C), 24.2, 24.4, 25.5, 25.7, 30.5, 32.3, 36.2, 36.8, 37.0, 119.0, 124.9, 131.1. HRMS (FAB) calcd for $C_{15}H_{28}N$ (MH^+): 222.2216; found: 222.2224.

(3*S*,7*R*)-3,7,11-Trimethyldodec-10-en-1-ol (6)[6]
To a stirred solution of **5** (1.00 g, 4.52 mmol) in CH_2Cl_2 (5.0 mL) was added dropwise 1.0 M DIBAL-H in THF (4.97 mL, 4.97 mmol) at −78 °C under argon. After the mixture was stirred for 2 h, saturated aqueous solution of sodium potassium tartrate was added and the mixture was warmed to room temperature. The whole was extracted with Et_2O and the extract was dried over $MgSO_4$. The extract was concentrated under reduced pressure after filtration through a short pad of silica gel to give crude aldehyde. To a stirred solution of the aldehyde in CH_2Cl_2 (5.0 mL) was added dropwise DIBAL-H in THF (1.0 M, 4.97 mL, 4.97 mmol) at −78 °C under argon. After the mixture was stirred for 2 h, saturated aqueous solution of sodium potassium tartrate was added. The whole was extracted with Et_2O and the extract was dried over $MgSO_4$. The extract was concentrated under reduced pressure, and the residue was purified by column chromatography to give the title alcohol **6** as a colorless oil (0.848 g, 83%). $[\alpha]_D^{25}$ −2.3 (*c* 0.90, $CHCl_3$); IR (neat): 3299 (OH), 1058 (C-O); ^{1}H NMR (500 MHz, $CDCl_3$) δ 0.86 (d, *J* = 6.3 Hz, 3H), 0.90 (d, *J* = 6.3 Hz, 3H), 1.07–1.41 (m, 11H), 1.54–1.64 (m, 1H), 1.61 (s, 3H), 1.69 (s, 3H), 1.89-2.03 (m, 2H), 3.64–3.73 (m, 2H), 5.09–5.11 (m, 1H); ^{13}C NMR (125 MHz, $CDCl_3$) δ 17.6, 19.6, 19.7, 24.3, 25.6, 25.7, 29.5, 32.4, 37.0, 37.2, 37.5, 40.0, 61.3, 125.0, 124.9, 131.0. HRMS (FAB) calcd for $C_{15}H_{31}O$ (MH^+): 227.2369; found: 227.2363.

(3*R*,7*S*)-3,7,11-Trimethyldodec-10-en-1-ol (*ent*-6)
According to the procedure described for the preparation of **6**, compound *ent*-**5** (900 mg, 4.07 mmol) was converted into *ent*-**6** as a colorless oil (606 mg, 66%).

$[\alpha]_D^{25}$ +2.0 (*c* 1.05, $CHCl_3$); IR (neat): 3299 (OH), 1055 (C–O); ^{1}H NMR (500 MHz, $CDCl_3$) δ 0.86 (d, J = 6.3 Hz, 3H), 0.90 (d, J = 6.3 Hz, 3H), 1.04–1.41 (m, 11H), 1.52–1.63 (m, 1H), 1.60 (s, 3H), 1.68 (s, 3H), 1.89–2.03 (m, 2H), 3.64–3.73 (m, 2H), 5.08–5.12 (m, 1H); ^{13}C NMR (125 MHz, $CDCl_3$) δ 17.6, 19.6, 19.7, 24.3, 25.6, 25.7, 29.5, 32.4, 37.0, 37.2, 37.5, 39.9, 61.3, 125.0, 124.9, 131.0. HRMS (FAB) calcd for $C_{15}H_{31}O$ (MH^+): 227.2369; found: 227.2363.

(6*R*,10*S*)-12-Bromo-2,6,10-trimethyldodec-2-ene (7)
To a stirred solution of compound **6** (800 mg, 3.53 mmol) in pyridine (2.70 mL) was added TsCl (876 mg, 4.60 mmol) at 0 °C. After the mixture was stirred for 2 h, saturated aqueous solution of citric acid was added. The whole was extracted with Et_2O and the extract was washed with H_2O and brine, and dried over $MgSO_4$. The extract was concentrated under reduced pressure after filtration through a short pad of silica gel to give a crude sulfonate. To a stirred solution of the sulfonate in acetone (5 mL) was added LiBr (1.80 g, 17.7 mmol). After the mixture was stirred for 1 h under reflux, the whole was concentrated under reduced pressure. To the residue was added H_2O and the whole was extracted with Et_2O and dried over $MgSO_4$. The filtrate was concentrated under reduced pressure, and the residue was purified by column chromatography to give the title bromide **7** as a colorless oil (923 mg, 90%). $[\alpha]_D^{25}$ +5.8 (*c* 1.00, $CHCl_3$); ^{1}H NMR (500 MHz, $CDCl_3$) δ 0.86 (d, J = 6.9 Hz, 3H), 0.89 (d, J = 6.9 Hz, 3H), 1.04–1.41 (m, 9H), 1.61 (s, 3H), 1.68 (s, 3H), 1.61–1.68 (m, 2H), 1.85–2.03 (m, 3H), 3.38-3.49 (m, 2H), 5.09–5.11 (m, 1H); ^{13}C NMR (125 MHz, $CDCl_3$) δ 17.6, 19.0, 19.6, 24.1, 25.6, 25.7, 31.6, 32.3, 32.4, 36.8, 37.1 (2C), 40.0, 125.0, 131.0. Anal. calcd. for $C_{15}H_{29}Br$: C, 62.28; H, 10.10. Found: C, 62.31; H, 10.32.

(6*S*,10*R*)-12-Bromo-2,6,10-trimethyldodec-2-ene (*ent*-7)
According to the procedure described for the preparation of **7**, compound *ent*-**6** (580 mg, 2.56 mmol) was converted into *ent*-**7** as a colorless oil (669 mg, 90%). $[\alpha]_D^{25}$ −5.8 (*c* 1.01, $CHCl_3$); ^{1}H NMR (500 MHz, $CDCl_3$) δ 0.86 (d, J = 6.9 Hz, 3H), 0.89 (d, J = 6.9 Hz, 3H), 1.07–1.41 (m, 9H), 1.61 (s, 3H), 1.68 (s, 3H), 1.61–1.68 (m, 2H), 1.84–2.03 (m, 3H), 3.38–3.49 (m, 2H), 5.09–5.11 (m, 1H); ^{13}C NMR (125 MHz, $CDCl_3$) δ 17.6, 19.0, 19.6, 24.1, 25.6, 25.7, 31.6, 32.2, 32.4, 36.8, 37.1 (2C), 40.0, 125.0, 131.0. Anal. calcd. for $C_{15}H_{29}Br$: C, 62.28; H, 10.10. Found: C, 62.22; H, 10.08.

Triphenyl((3*S*,7*R*)-3,7,11-trimethyldodec-10-en-1-yl)phosphonium Bromide (8)
A mixture of the bromide **7** (757 mg, 2.61 mmol) and PPh_3 (750 mg, 2.87 mmol) was heated to 100 °C and the mixture was stirred for 15 h. After cooling, Et_2O was added to the mixture and the resulting white precipitate was washed with Et_2O to remove the excess PPh_3. The residue was dried under vacuum to give the title phosphonium salt **8**, which was used without further purification.

Triphenyl((3*S*,7*R*)-3,7,11-trimethyldodec-10-en-1-yl)phosphonium Bromide (*ent*-8)
According to the procedure described for the preparation of **8**, compound *ent*-**7** (600 mg, 2.07 mmol) was converted into *ent*-**8**.

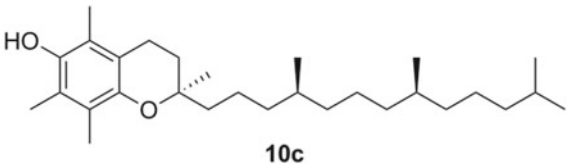
(*S*)-2,5,7,8-Tetramethyl-2-((4*S*,8*S*)-4,8,12-trimethyltridecyl)chroman-6-ol (10b) [22]

To a stirred solution of phosphonium salt **8** (ca. 2.61 mmol) in THF (15.0 mL) was added LHMDS (1.0 M, 2.30 mL, 2.30 mmol) in THF dropwise at −40 °C under argon. After the mixture was stirred for 30 min, the aldehyde **9** [23] (675 mg, 2.08 mmol) in THF (5.0 mL) was added to the mixture. The stirring was continued for 30 min at the same temperature and for 1 h at 0 °C. After the reaction was quenched with saturated aqueous solution of NH_4Cl, the whole was extracted with Et_2O and the extract was washed with H_2O and brine, and dried over Na_2SO_4. The filtrate was concentrated under reduced pressure. The oily residue was dissolved in hexane and the solution was filtrated through a short pad of silica gel to remove phosphine oxide and the filtrated was concentrated under reduced pressure. To a stirred solution of the crude alkene in TBME (9.5 mL) was added PtO_2 (37.8 mg, 0.167 mmol). The mixture was stirred under an atmosphere of H_2 at room temperature. After 30 min, the reaction mixture was filtrated through Celite and the filtrate was concentrated. To a stirred solution of the residue in MeOH (35.0 mL) was added 10% Pd/C (222 mg, 0.208 mmol). The mixture was stirred under an atmosphere of H_2 at room temperature. After 30 min, the reaction mixture was filtrated through Celite. The filtrate was concentrated under reduced pressure, and the residue was purified by column chromatography to give the title compound **10b** as a pale yellow oil (759 mg, 84%). $[\alpha]_D^{25}$ −0.7 (*c* 1.01, $CHCl_3$); ^{1}H NMR (500 MHz, $CDCl_3$) δ 0.83–0.87 (m, 12H), 1.02–1.53 (m, 21H), 1.23 (s, 3H), 1.73–1.84 (m, 2H), 2.11 (s, 6H), 2.16 (s, 3H), 2.60 (t, J = 6.9 Hz, 2H), 4.17 (s, 1H); ^{13}C NMR (125 MHz, $CDCl_3$) δ 11.3, 11.8, 12.2, 19.6, 19.7, 20.7, 21.0, 22.6, 22.7, 23.8, 24.4, 24.8, 28.0, 31.5, 32.7, 32.9, 37.3, 37.4 (3C), 39.4, 39.8, 74.5, 117.3, 118.4, 121.0, 122.6, 144.5, 145.5. HRMS (ESI) calcd for $C_{29}H_{50}O_2$ (M^+): 430.3811; found: 430.3806.

(*R*)-2,5,7,8-Tetramethyl-2-((4*S*,8*S*)-4,8,12-trimethyltridecyl)chroman-6-ol (10c)

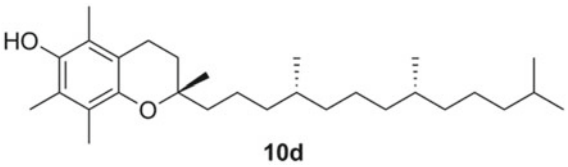
According to the procedure described for the preparation of **10b**, compound *ent*-**9** (675 mg, 2.07 mmol) was converted into compound **10c** by the reaction with **8** (ca. 2.61 mmol) as a pale yellow oil (573 mg, 57%) (Fig. 2.14). $[\alpha]_D^{25}$ +1.0 (*c* 1.10, $CHCl_3$); ^{1}H NMR (500 MHz, $CDCl_3$) δ 0.83–0.87 (m, 12H), 1.03–1.58 (m, 21H), 1.23 (s, 3H), 1.73–1.84 (m, 2H), 2.11 (s, 6H), 2.16 (s, 3H), 2.60 (t, J = 6.9 Hz, 2H), 4.17 (s, 1H); ^{13}C NMR (125 MHz, $CDCl_3$) δ 11.3, 11.8, 12.2, 19.7 (2C), 20.8, 21.0, 22.6, 22.7, 23.8, 24.4, 24.8, 28.0, 31.4, 32.7, 32.8, 37.3, 37.4 (2C), 37.5, 39.4, 39.8, 74.5, 117.3, 118.4, 121.0, 122.6, 144.5, 145.5. HRMS (ESI) calcd for $C_{29}H_{50}O_2$ (M^+): 430.3811; found: 430.3803.

Fig. 2.14 Structure of **10c**



10c

Fig. 2.15 Structure of **10d**



10d

(*S*)-2,5,7,8-Tetramethyl-2-((4*R*,8*R*)-4,8,12-trimethyltridecy)chroman-6-ol (10d) According to the procedure described for the preparation of **10b**, compound **9** (540 mg, 1.66 mmol) was converted into compound **10d** by the reaction with *ent*-**8** (ca. 2.08 mmol) as a pale yellow oil (573 mg, 80%) (Fig. 2.15). $[\alpha]_D^{25}$ −1.0 (*c* 1.00, $CHCl_3$); ^1H NMR (500 MHz, $CDCl_3$) δ 0.83–0.87 (m, 12H), 1.03–1.58 (m, 21H), 1.23 (s, 3H), 1.73-1.84 (m, 2H), 2.11 (s, 6H), 2.16 (s, 3H), 2.60 (t, J = 6.9 Hz, 2H), 4.17 (s, 1H); ^{13}C NMR (125 MHz, $CDCl_3$) δ 11.3, 11.8, 12.2, 19.7 (2C), 20.8, 21.0, 22.6, 22.7, 23.8, 24.4, 24.8, 28.0, 31.5, 32.7, 32.9, 37.3, 37.4 (2C), 37.5, 39.4, 39.8, 74.5, 117.3, 118.4, 121.0, 122.6, 144.5, 145.5. HRMS(ESI) calcd for $C_{29}H_{50}O_2$ (M^+): 430.3811; found: 430.3801.

1-(2,4-Dihydroxyphenyl)-2-{[(*S*)-2,5,7,8-tetramethyl-2-((4*S*,8*S*)-4,8,12-trimethyltridecyl)chroman-6-yl]oxy}ethan-1-one (12b)
To a stirred solution of compound **10b** (600 mg, 1.39 mmol) in DMF (1.4 mL) were added K_2CO_3 (385 mg, 2.78 mmol) and compound **11** (745 mg, 1.81 mmol) at room temperature. After the mixture was stirred overnight, the reaction was quenched with H_2O. The whole was extracted with Et_2O and the extract was washed with H_2O and brine, and dried over $MgSO_4$. The filtrate was concentrated under reduced pressure. To a stirred solution of the residue in EtOAc (15.0 mL) was added 10% Pd/C (149 mg, 0.140 mmol). The mixture was stirred under an atmosphere of H_2 at room temperature. After the reaction was completed, the reaction mixture was filtrated through Celite. Purification by column chromatography gave the title compound **12b** as pale yellow solid (583 mg, 72%): mp 87–88 °C; $[\alpha]_D^{25}$ −4.0 (*c* 1.01, $CHCl_3$); IR (neat): 3315 (OH), 1627 (C=O); ^1H NMR (500 MHz, $CDCl_3$) δ 0.84–0.87 (m, 12H), 1.04–1.57 (m, 21H), 1.24 (s, 3H), 1.73–1.85 (m, 2H), 2.09 (s, 3H), 2.14 (s, 3H), 2.18 (s, 3H), 2.58 (t, J = 6.6 Hz, 2H), 4.92 (s, 2H), 5.80 (br s, 1H), 6.36 (dd, J = 8.6, 2.3 Hz, 1H), 6.42 (d, J = 2.3 Hz, 1H), 7.52 (d, J = 7.7 Hz, 1H), 12.40 (s, 1H); ^{13}C NMR (125 MHz, $CDCl_3$) δ 11.8, 11.9, 12.8, 19.7 (2C), 20.6, 21.0, 22.6, 22.7, 23.8, 24.4, 24.8, 28.0, 31.2, 32.7, 32.8, 37.3, 37.4 (3C), 39.4, 40.0, 74.0, 75.0, 103.8, 108.0, 111.9, 117.8, 123.2, 125.7, 127.6, 130.9, 147.8, 148.3, 162.8, 165.3, 198.0. Anal. calcd. for $C_{37}H_{56}O_5$: C, 76.51; H, 9.72. Found: C, 76.41; H, 9.89.

1-(2,4-Dihydroxyphenyl)-2-{[(*R*)-2,5,7,8-tetramethyl-2-((4*S*,8*S*)-4,8,12-trimethyltridecyl)chroman-6-yl]oxy}ethan-1-one (12c)
According to the procedure described for the preparation of **12b**, compound **10c** (100 mg, 0.232 mmol) was converted into compound **12c** as pale yellow solid (88.9 mg, 66%) (Fig. 2.16): mp 86–87 °C; $[\alpha]_D^{25}$ +3.7 (*c* 0.55, $CHCl_3$); IR (neat):

Fig. 2.16 Structure of **12c**

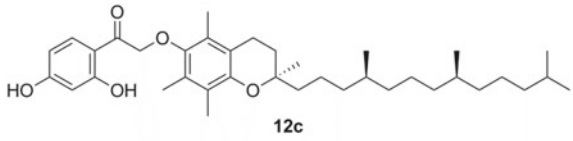
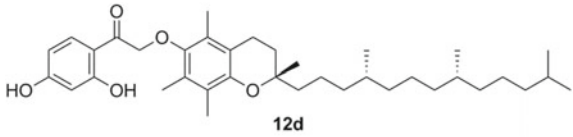


Fig. 2.17 Structure of **12d**



3351 (OH), 1626 (C=O); ^{1}H NMR (500 MHz, $CDCl_3$) δ 0.84–0.87 (m, 12H), 1.04–1.61 (m, 21H), 1.24 (s, 3H), 1.73–1.85 (m, 2H), 2.08 (s, 3H), 2.14 (s, 3H), 2.18 (s, 3H), 2.58 (t, J = 6.9 Hz, 2H), 4.92 (s, 2H), 6.36 (dd, J = 8.9, 2.6 Hz, 1H), 6.42 (d, J = 2.9 Hz, 1H), 7.51 (d, J = 9.2 Hz, 1H), 12.40 (s, 1H); ^{13}C NMR (125 MHz, $CDCl_3$) δ 11.8, 11.9, 12.8, 19.7 (2C), 20.6, 21.0, 22.6, 22.7, 23.8, 24.4, 24.8, 28.0, 31.1, 32.7, 32.8, 37.3, 37.4 (2C), 37.5, 39.4, 40.1, 74.0, 75.0, 103.8, 108.1, 111.9, 117.8, 123.2, 125.7, 127.6, 130.9, 147.8, 148.3, 162.9, 165.3, 198.0. Anal. Calcd. for $C_{37}H_{56}O_5$: C, 76.51; H, 9.72. Found: C, 76.35; H, 9.79.

1-(2,4-Dihydroxyphenyl)-2-{[(*S*)-2,5,7,8-tetramethyl-2-((4*R*,8*R*)-4,8,12-trimethyltridecyl)chroman-6-yl]oxy}ethan-1-one (12d)
According to the procedure described for the preparation of **12b**, compound **10d** (500 mg, 1.16 mmol) was converted into compound **12d** as pale yellow solid (483 mg, 72%) (Fig. 2.17): mp 86–87 °C; $[\alpha]_D^{25}$ −3.9 (*c* 1.11, $CHCl_3$); IR (neat): 3350 (OH), 1626 (C=O); ^{1}H NMR (500 MHz, $CDCl_3$) δ 0.84–0.87 (m, 12H), 1.04–1.61 (m, 21H), 1.24 (s, 3H), 1.73–1.85 (m, 2H), 2.08 (s, 3H), 2.14 (s, 3H), 2.18 (s, 3H), 2.58 (t, J = 6.9 Hz, 2H), 4.92 (s, 2H), 6.36 (dd, J = 8.9, 2.6 Hz, 1H), 6.42 (d, J = 2.9 Hz, 1H), 7.51 (d, J = 9.2 Hz, 1H), 12.40 (s, 1H); ^{13}C NMR (125 MHz, $CDCl_3$) δ 11.8, 11.9, 12.8, 19.7 (2C), 20.6, 21.0, 22.6, 22.7, 23.8, 24.4, 24.8, 28.0, 31.1, 32.7, 32.8, 37.3, 37.4 (2C), 37.5, 39.4, 40.1, 74.0, 75.0, 103.8, 108.1, 111.8, 117.8, 123.2, 125.7, 127.6, 130.9, 147.7, 148.3, 163.0, 165.3, 198.0. HRMS (ESI) calcd for $C_{37}H_{57}O_5$ (MH^+): 581.4201; found: 581.4207.

7-Hydroxy-3-{[(*R*)-2,5,7,8-tetramethyl-2-((4*R*,8*R*)-4,8,12-trimethyltridecyl)chroman-6-yl]oxy}-4*H*-chromen-4-one (1a, NP843)
mp 228–229 °C; $[\alpha]_D^{25}$ +5.0 (*c* 1.00, $CHCl_3$); IR (neat): 3163 (OH); ^{1}H NMR (500 MHz, $CDCl_3$) δ 0.84–0.87 (m, 12H), 1.03–1.59 (m, 21H), 1.25 (s, 3H), 1.75–1.85 (m, 2H), 2.02 (s, 3H), 2.06 (s, 3H), 2.09 (s, 3H), 2.58 (t, J = 6.9 Hz, 2H), 6.86 (d, J = 2.3 Hz, 1H), 7.07–7.10 (m, 2H), 8.22 (d, J = 9.2 Hz, 1H), 8.67 (br s, 1H); ^{13}C NMR (125 MHz, $CDCl_3$) δ 11.8 (2C), 12.6, 19.6, 19.7, 20.6, 21.0, 22.6, 22.7, 23.7, 24.4, 24.8, 28.0, 31.2, 32.7, 32.8, 37.3, 37.4 (3C), 39.4, 40.0, 75.3, 102.7, 115.5, 117.0, 118.2, 123.7, 125.3, 127.1, 127.6, 140.0, 142.8, 143.4, 149.0, 157.8, 162.2, 172.6. Anal. calcd. for $C_{38}H_{54}O_5$: C, 77.25; H, 9.21. Found: C, 77.13; H, 9.40.

7-Hydroxy-3-{[(*S*)-2,5,7,8-tetramethyl-2-((4*S*,8*S*)-4,8,12-trimethyltridecyl])chroman-6-yl]oxy}-4*H*-chromen-4-one (1b)

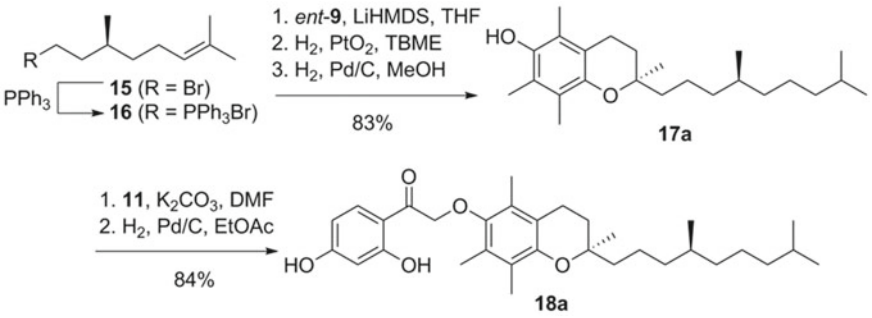
To a stirred solution of compound **12** (100 mg, 0.172 mmol) in THF (0.76 mL) was added DMF-DMA (27.7 μL, 0.260 mmol) under argon, and the mixture was stirred under reflux for 4 h. Then, aqueous 1N HCl (1 mL) and MeOH (1 mL) were added and the mixture was stirred overnight. The whole was extracted with Et_2O and dried over Na_2SO_4. The filtrate was concentrated under reduced pressure, and the residue was purified by column chromatography to give the title compound **1b** as white solid (23.3 mg, 23%): mp 228–229 °C; $[\alpha]_D^{25}$ −5.3 (*c* 1.00, $CHCl_3$); IR (neat): 3133 (OH); ^{1}H NMR (500 MHz, $CDCl_3$) δ 0.84–0.87 (m, 12H), 1.03–1.59 (m, 21H), 1.25 (s, 3H), 1.75–1.85 (m, 2H), 2.02 (s, 3H), 2.06 (s, 3H), 2.09 (s, 3H), 2.58 (t, *J* = 6.9 Hz, 2H), 6.86 (d, *J* = 2.3 Hz, 1H), 7.07–7.10 (m, 2H), 8.22 (d, *J* = 9.2 Hz, 1H), 8.55 (br s, 1H); ^{13}C NMR (125 MHz, $CDCl_3$) δ 11.8 (2C), 12.6, 19.6, 19.7, 20.6, 21.0, 22.6, 22.7, 23.8, 24.4, 24.8, 28.0, 31.2, 32.7, 32.8, 37.3, 37.4 (3C), 39.4, 40.0, 75.2, 102.7, 115.5, 117.0, 118.2, 123.7, 125.3, 127.1, 127.6, 140.0, 142.8, 143.4, 149.0, 157.8, 162.1, 172.6. Anal. calcd. for $C_{38}H_{54}O_5$: C, 77.25; H, 9.21. Found: C, 77.22; H, 9.43.

7-Hydroxy-3-{[(*R*)-2,5,7,8-tetramethyl-2-((4*S*,8*S*)-4,8,12-trimethyltridecyl])chroman-6-yl]oxy}-4*H*-chromen-4-one (1c)

According to the procedure described for the preparation of **1b**, compound **12c** (50.0 mg, 0.0861 mmol) was converted into compound **1c** as white solid (12.2 mg, 24%): mp 229–231 °C; $[\alpha]_D^{25}$ +5.4 (*c* 1.01, $CHCl_3$); IR (neat): 3125 (OH); ^{1}H NMR (500 MHz, $CDCl_3$) δ 0.84–0.87 (m, 12H), 1.03–1.64 (m, 21H), 1.25 (s, 3H), 1.75–1.85 (m, 2H), 2.02 (s, 3H), 2.06 (s, 3H), 2.09 (s, 3H), 2.58 (t, *J* = 6.9 Hz, 2H), 6.86 (d, *J* = 2.3 Hz, 1H), 7.07–7.10 (m, 2H), 8.22 (d, *J* = 8.6 Hz, 1H), 8.57 (br s, 1H); ^{13}C NMR (125 MHz, $CDCl_3$) δ 11.8 (2C), 12.6, 19.7 (2C), 20.6, 21.0, 22.6, 22.7, 23.7, 24.4, 24.8, 28.0, 31.1, 32.7, 32.8, 37.3, 37.4 (3C), 39.4, 40.0, 75.3, 102.7, 115.5, 117.0, 118.3, 123.7, 125.3, 127.1, 127.6, 140.0, 142.8, 143.4, 149.1, 157.8, 162.1, 172.6. Anal. calcd. for $C_{38}H_{54}O_5 \cdot 0.15$EtOAc: C, 76.75; H, 9.21. Found: C, 76.40; H, 9.21.

7-Hydroxy-3-{[(*S*)-2,5,7,8-tetramethyl-2-((4*R*,8*R*)-4,8,12-trimethyltridecyl])chroman-6-yl]oxy}-4*H*-chromen-4-one (1d)

According to the procedure described for the preparation of **1b**, compound **12d** (100 mg, 0.172 mmol) was converted into compound **1d** as white solid (23.5 mg, 23%): mp 229–231 °C; $[\alpha]_D^{25}$ −5.4 (*c* 0.95, $CHCl_3$); IR (neat): 3126 (OH); ^{1}H NMR (500 MHz, $CDCl_3$) δ 0.84–0.87 (m, 12H), 1.03–1.64 (m, 21H), 1.25 (s, 3H), 1.75–1.85 (m, 2H), 2.02 (s, 3H), 2.06 (s, 3H), 2.09 (s, 3H), 2.58 (t, *J* = 6.9 Hz, 2H), 6.86 (d, *J* = 2.3 Hz, 1H), 7.07–7.10 (m, 2H), 8.22 (d, *J* = 8.6 Hz, 1H), 8.51 (br s, 1H); ^{13}C NMR (125 MHz, $CDCl_3$) δ 11.8 (2C), 12.6, 19.7 (2C), 20.6, 21.0, 22.6, 22.7, 23.8, 24.4, 24.8, 28.0, 31.1, 32.7, 32.8, 37.3, 37.4 (3C), 39.4, 40.0, 75.3, 102.7, 115.4, 117.0, 118.3, 123.7, 125.3, 127.1, 127.6, 139.9, 142.8, 143.4, 149.1, 157.8, 162.1, 172.6. Anal. calcd. for $C_{38}H_{54}O_5$: C, 77.25; H, 9.21. Found: C, 77.36; H, 9.32.



Scheme 2.3 Synthetic scheme for **18a**

(*S*)-(3,7-Dimethyloct-6-en-1-yl)triphenylphosphonium Bromide (16)
According to the procedure described for the preparation of **8**, (*S*)-citronellyl bromide **15** (3.99 g, 18.2 mmol) was converted into compound **16**, which was used without further purification.

(*R*)-2-((*S*)-4,8-Dimethylnonyl)-2,5,7,8-tetramethylchroman-6-ol (17a)
According to the procedure described for the preparation of **10b**, compound *ent*-**9** (800 mg, 2.47 mmol) was converted into compound **17a** using the phosphonium salt **16** (ca. 4.93 mmol) as a pale yellow oil (735 mg, 83%) (Scheme 2.3). $[\alpha]_D^{25}$ +0.4 (*c* 1.00, $CHCl_3$); ^{1}H NMR (500 MHz, $CDCl_3$) δ 0.83–0.88 (m, 9H), 1.05–1.53 (m, 14H), 1.23 (s, 3H), 1.73–1.84 (m, 2H), 2.11 (s, 6H), 2.16 (s, 3H), 2.60 (t, J = 6.9 Hz, 2H), 4.18 (s, 1H); ^{13}C NMR (125 MHz, $CDCl_3$) δ 11.3, 11.8, 12.2, 19.7 (2C), 21.0, 22.6, 22.7, 23.8, 24.7, 28.0, 31.5, 32.7, 37.2, 37.5, 39.3, 39.8, 74.5, 117.3, 118.4, 121.0, 122.6, 144.5, 145.5. HRMS (ESI) calcd for $C_{24}H_{40}O_2$ (M^+): 360.3028; found: 360.3026.

(*S*)-2-((*S*)-4,8-Dimethylnonyl)-2,5,7,8-tetramethylchroman-6-ol (17b)
According to the procedure described for the preparation of **10b**, compound **9** (800 mg, 2.47 mmol) was converted into compound **17b** using phosphonium salt **16** (ca. 4.93 mmol) as a pale yellow oil (730 mg, 82%). $[\alpha]_D^{25}$ +1.5 (*c* 1.00, $CHCl_3$); ^{1}H NMR (500 MHz, $CDCl_3$) δ 0.83–0.88 (m, 9H), 1.04–1.53 (m, 14H), 1.23 (s, 3H), 1.73–1.84 (m, 2H), 2.11 (s, 6H), 2.16 (s, 3H), 2.60 (t, J = 6.9 Hz, 2H), 4.18 (s, 1H); ^{13}C NMR (125 MHz, $CDCl_3$) δ 11.3, 11.8, 12.2, 19.6, 20.7, 21.0, 22.6, 22.7, 23.8, 24.8, 28.0, 31.5, 32.7, 37.3, 37.5, 39.3, 39.7, 74.5, 117.3, 118.4, 121.0, 122.6, 144.5, 145.5. HRMS (ESI) calcd for $C_{24}H_{40}O_2$ (M^+): 360.3028; found: 360.3035.

1-(2,4-Dihydoxyphenyl)-2-{[(*R*)-2-((*S*)-4,8-dimethylnonyl)-2,5,7,8-tetramethylchroman-6-yl]oxy}ethan-1-one (18a)
According to the procedure described for the preparation of **12b**, compound **17a** (700 mg, 1.94 mmol) was converted into compound **18a** as a pale yellow solid (916 mg, 84%): mp 89–91 °C; $[\alpha]_D^{25}$ +3.8 (*c* 0.70, $CHCl_3$); IR (neat): 3341 (OH), 1626 (C=O); ^{1}H NMR (500 MHz, $CDCl_3$) δ 0.84–0.87 (m, 9H), 1.06–1.61 (m, 14H), 1.24 (s, 3H), 1.73–1.85 (m, 2H), 2.09 (s, 3H), 2.14 (s, 3H), 2.18 (s, 3H), 2.57

(t, J = 6.6 Hz, 2H), 4.93 (s, 2H), 6.37 (dd, J = 8.9, 2.6 Hz, 1H), 6.42 (d, J = 2.9 Hz, 1H), 7.49 (d, J = 8.6 Hz, 1H), 12.37 (s, 1H); ^{13}C NMR (125 MHz, $CDCl_3$) δ 11.8, 11.9, 12.8, 19.6, 20.6, 21.0, 22.6, 22.7, 23.8, 24.7, 28.0, 31.1, 32.7, 37.2, 37.5, 39.3, 40.0, 73.9, 75.0, 103.8, 108.2, 111.7, 117.8, 123.2, 125.7, 127.6, 130.8, 147.7, 148.3, 163.2, 165.3, 198.0. HRMS (ESI) calcd for $C_{32}H_{47}O_5$ (MH^+): 511.3418; found: 511.3414.

1-(2,4-Dihydroxyphenyl)-2-{[(*S*)-2-((*S*)-4,8-dimethylnonyl)-2,5,7,8-tetramethylchroman-6-yl]oxy}ethan-1-one (18b)

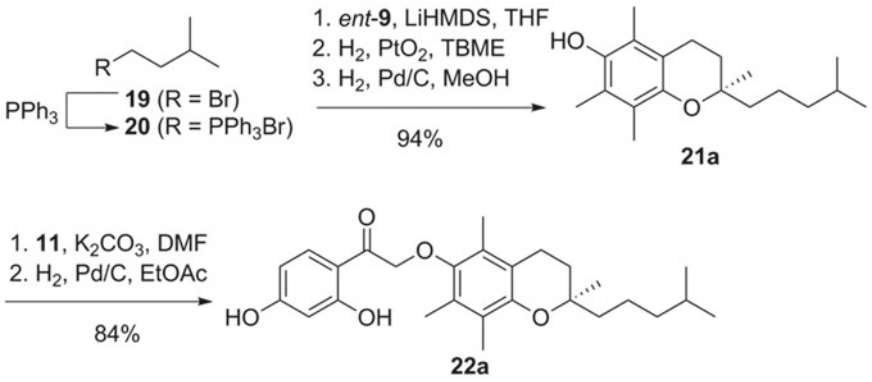
According to the procedure described for the preparation of **12b**, compound **17b** (700 mg, 1.94 mmol) was converted into compound **18b** as a pale yellow solid (766 mg, 79%): mp 89–91 °C; $[\alpha]_D^{25}$ −3.7 (*c* 0.62, $CHCl_3$); IR (neat): 3363 (OH), 1626 (C=O); ^{1}H NMR (500 MHz, $CDCl_3$) δ 0.84-0.87 (m, 9H), 1.03–1.60 (m, 14H), 1.24 (s, 3H), 1.73–1.85 (m, 2H), 2.09 (s, 3H), 2.14 (s, 3H), 2.18 (s, 3H), 2.57 (t, J = 6.6 Hz, 2H), 4.93 (s, 2H), 6.26 (s, 1H), 6.37 (dd, J = 9.2, 2.3 Hz, 1H), 6.42 (d, J = 2.9 Hz, 1H), 7.50 (d, J = 9.2 Hz, 1H), 12.38 (s, 1H); ^{13}C NMR (125 MHz, $CDCl_3$) δ 11.8, 11.9, 12.8, 19.6, 20.6, 21.0, 22.6, 22.7, 23.8, 24.7, 28.0, 31.2, 32.7, 37.3, 37.5, 39.3, 40.0, 73.9, 75.0, 103.8, 108.2, 111.7, 117.8, 123.2, 125.7, 127.6, 130.9, 147.7, 148.3, 163.1, 165.3, 198.0. HRMS (ESI) calcd for $C_{32}H_{47}O_5$ (MH^+): 511.3418; found: 511.3419.

3-{[(*R*)-2-((*S*)-4,8-Dimethylnonyl)-2,5,7,8-tetramethylchroman-6-yl]oxy}-7-hydroxy-4*H*-chromen-4-one (13a)

According to the procedure described for the preparation of **1b**, compound **18a** (100 mg, 0.196 mmol) was converted into compound **13a** as a white solid (20.5 mg, 20%): mp 239–241 °C; $[\alpha]_D^{25}$ +5.4 (*c* 0.33, $CHCl_3$); IR (neat): 3116 (OH); ^{1}H NMR (500 MHz, $CDCl_3$) δ 0.84–0.87 (m, 9H), 1.06–1.61 (m, 14H), 1.25 (s, 3H), 1.75–1.85 (m, 2H), 2.02 (s, 3H), 2.05 (s, 3H), 2.09 (s, 3H), 2.58 (t, J = 6.7 Hz, 2H), 6.86 (d, J = 2.3 Hz, 1H), 7.07–7.10 (m, 2H), 8.22 (d, J = 8.7 Hz, 1H), 8.59 (br s, 1H); ^{13}C NMR (125 MHz, $CDCl_3$) δ 11.8 (2C), 12.7, 19.6, 20.6, 21.0, 22.6, 22.7, 23.8, 24.7, 28.0, 31.1, 32.7, 37.2, 37.5, 39.3, 39.9, 75.3, 102.7, 115.5, 117.0, 118.3, 123.7, 125.3, 127.1, 127.6, 140.0, 142.8, 143.4, 149.0, 157.8, 162.1, 172.6. Anal. calcd. for $C_{33}H_{44}O_5 \cdot 0.25$EtOAc: C, 75.24; H, 8.54. Found: C, 75.08; H, 8.60.

3-{[(*S*)-2-((*S*)-4,8-Dimethylnonyl)-2,5,7,8-tetramethylchroman-6-yl]oxy}-7-hydroxy-4*H*-chromen-4-one (13b)

According to the procedure described for the preparation of **1b**, compound **18b** (100 mg, 0.196 mmol) was converted into compound **13b** as a white solid (23.4 mg, 23%): mp 239–241 °C; $[\alpha]_D^{25}$ −5.6 (*c* 0.39, $CHCl_3$); IR (neat): 3131 (OH); ^{1}H NMR (500 MHz, $CDCl_3$) δ 0.86 (d, J = 6.3 Hz, 9H), 1.05–1.59 (m, 14H), 1.25 (s, 3H), 1.76–1.84 (m, 2H), 2.02 (s, 3H), 2.06 (s, 3H), 2.09 (s, 3H), 2.58 (t, J = 6.9 Hz, 2H), 6.85 (d, J = 1.7 Hz, 1H), 7.07 (dd, J = 9.2, 2.3 Hz, 1H), 7.09 (s, 1H), 8.22 (d, J = 8.6 Hz, 1H), 8.38 (br s, 1H); ^{13}C NMR (125 MHz, $CDCl_3$) δ 11.8 (2C), 12.6, 19.6, 20.6, 21.0, 22.6, 22.7, 23.7, 24.7, 28.0, 31.2, 32.7, 37.3, 37.5, 39.3, 39.9, 75.3, 102.7, 115.7, 116.7, 118.3, 123.6, 125.3, 127.1, 127.4, 140.2, 142.8, 143.3, 149.0, 157.9, 162.5, 172.7. Anal. calcd. For $C_{33}H_{44}O_5 \cdot 0.1$EtOAc: C, 75.76; H, 8.53. Found: C, 75.65; H, 8.58.



Scheme 2.4 Synthetic scheme for **22a**

(Isopentyl)triphenylphosphonium Bromide (19)
According to the procedure described for the preparation of **8**, 1-bromo-3-methylbutane **19** (1.99 g, 13.2 mmol) was converted into compound **20**, which was used without further purification.

(*R*)-2,5,7,8-Tetramethyl-2-(4-methylpentyl)chroman-6-ol (21a)
According to the procedure described for the preparation of **10b**, compound *ent*-**9** (800 mg, 2.47 mmol) was converted into compound **21a** using the phosphonium salt **20** (ca. 4.93 mmol) as a pale yellow oil (675 mg, 94%) (Scheme 2.4). $[\alpha]_D^{25}$ −0.9 (*c* 1.00, $CHCl_3$); ^{1}H NMR (500 MHz, $CDCl_3$) δ 0.87 (d, J = 6.9 Hz, 6H), 1.14–1.19 (m, 2H), 1.22 (s, 3H), 1.37–1.58 (m, 5H), 1.73–1.84 (m, 2H), 2.11 (s, 6H), 2.16 (s, 3H), 2.60 (t, J = 6.9 Hz, 2H), 4.17 (s, 1H); ^{13}C NMR (125 MHz, $CDCl_3$) δ 11.3, 11.8, 12.2, 20.7, 21.4, 22.6 (2C), 23.8, 27.9, 31.5, 39.4, 39.7, 74.5, 117.3, 118.4, 121.0, 122.6, 144.5, 145.5. HRMS (ESI) calcd for $C_{19}H_{30}O_2$ (M^+): 290.2246; found: 290.2245.

(*S*)-2,5,7,8-Tetramethyl-2-(4-methylpentyl)chroman-6-ol (21b)
According to the procedure described for the preparation of **10b**, compound **9** (800 mg, 2.47 mmol) was converted into compound **21b** using compound **20** (ca. 4.93 mmol) as a pale yellow oil (621 mg, 86%). $[\alpha]_D^{25}$ +0.9 (*c* 1.00, $CHCl_3$); ^{1}H NMR (500 MHz, $CDCl_3$) δ 0.87 (d, J = 6.9 Hz, 6H), 1.14–1.19 (m, 2H), 1.22 (s, 3H), 1.37–1.58 (m, 5H), 1.73–1.84 (m, 2H), 2.11 (s, 6H), 2.16 (s, 3H), 2.60 (t, J = 6.9 Hz, 2H), 4.17 (s, 1H); ^{13}C NMR (125 MHz, $CDCl_3$) δ 11.3, 11.8, 12.2, 20.7, 21.4, 22.6 (2C), 23.8, 27.9, 31.5, 39.4, 39.7, 74.5, 117.3, 118.4, 121.0, 122.6, 144.5, 145.5. HRMS (ESI) calcd for $C_{19}H_{30}O_2$ (M^+): 290.2246; found: 290.2239.

(*R*)-1-(2,4-Dihydroxyphenyl)-2-{[2,5,7,8-tetramethyl-2-(4-methylpentyl)chroman-6-yl]oxy}ethan-1-one (22a)
According to the procedure described for the preparation of **12b**, compound **21a** (600 mg, 2.07 mmol) was converted into compound **22a** as a pale yellow solid (765 mg, 84%): mp 86–87 °C; $[\alpha]_D^{25}$ +3.5 (*c* 0.78, $CHCl_3$); IR (neat): 3351 (OH), 1626 (C=O); ^{1}H NMR (500 MHz, $CDCl_3$) δ 0.87 (d, J = 6.9 Hz, 6H), 1.18 (dd,

J = 14.9, 6.9 Hz, 2H), 1.24 (s, 3H), 1.37–1.61 (m, 5H), 1.73–1.85 (m, 2H), 2.08 (s, 3H), 2.14 (s, 3H), 2.18 (s, 3H), 2.57 (t, *J* = 6.6 Hz, 2H), 4.93 (s, 2H), 6.36 (dd, *J* = 8.9, 2.3 Hz, 1H), 6.42 (d, *J* = 2.3 Hz, 1H), 6.52 (br s, 1H), 7.49 (d, *J* = 9.2 Hz, 1H), 12.37 (s, 1H); ^{13}C NMR (125 MHz, $CDCl_3$) δ 11.8, 11.9, 12.8, 20.6, 21.3, 22.6 (2C), 23.8, 27.8, 31.1, 39.3, 39.9, 73.9, 75.0, 103.8, 108.1, 111.7, 117.8, 123.2, 125.7, 127.6, 130.8, 147.7, 148.3, 163.3, 165.3, 198.0. HRMS (ESI) calcd for $C_{27}H_{37}O_5$ (MH^+): 441.2636; found: 441.2633.

(*S*)-1-(2,4-Dihydroxyphenyl)-2-{[2,5,7,8-tetramethyl-2-(4-methylpentyl)chroman-6-yl]oxy}ethan-1-one (22b)

According to the procedure described for the preparation of **12b**, compound **21b** (600 mg, 2.07 mmol) was converted into compound **22b** as pale yellow solid (505 mg, 55%): mp 86–87 °C; $[\alpha]_D^{25}$ −3.9 (*c* 1.11, $CHCl_3$); IR (neat): 3351 (OH), 1626 (C=O); ^{1}H NMR (500 MHz, $CDCl_3$) δ 0.87 (d, *J* = 6.9 Hz, 6H), 1.17 (dd, *J* = 14.9, 6.9 Hz, 2H), 1.24 (s, 3H), 1.37–1.61 (m, 5H), 1.73–1.85 (m, 2H), 2.09 (s, 3H), 2.14 (s, 3H), 2.18 (s, 3H), 2.57 (t, *J* = 6.6 Hz, 2H), 4.93 (s, 2H), 6.28 (br s, 1H), 6.37 (dd, *J* = 8.9, 2.3 Hz, 1H), 6.42 (d, *J* = 2.3 Hz, 1H), 7.50 (d, *J* = 9.2 Hz, 1H), 12.38 (s, 1H); ^{13}C NMR (125 MHz, $CDCl_3$) δ 11.8, 11.9, 12.8, 20.6, 21.3, 22.6 (2C), 23.8, 27.8, 31.1, 39.3, 39.9, 73.9, 75.0, 103.8, 108.1, 111.7, 117.8, 123.2, 125.7, 127.6, 130.8, 147.7, 148.3, 163.1, 165.3, 198.0. Anal. calcd. for $C_{27}H_{36}O_5$: C, 73.61; H, 8.24. Found: C, 73.39; H, 8.49.

(*R*)-7-Hydroxy-3-{[2,5,7,8-tetramethyl-2-(4-methylpentyl)chroman-6-yl]oxy}-4*H*-chromen-4-one (14a)

According to the procedure described for the preparation of **1b**, compound **22a** (100 mg, 0.227 mmol) was converted into compound **14a** as white solid (23.0 mg, 23%): mp 255–258 °C; $[\alpha]_D^{25}$ +5.3 (*c* 0.40, THF); IR (neat): 3265 (OH); ^{1}H NMR (500 MHz, THF-d_8) δ 2.69 (d, *J* = 2.9 Hz, 3H), 2.70 (d, *J* = 2.9 Hz, 3H), 3.01 (dd, *J* = 14.9, 6.9 Hz, 2H), 3.06 (s, 3H), 3.26–3.43 (m, 5H), 3.56–3.68 (m, 2H), 3.82 (s, 3H), 3.86 (s, 3H), 3.89 (s, 3H), 4.44 (t, *J* = 6.9 Hz, 2H), 8.47 (d, *J* = 2.3 Hz, 1H), 8.64 (dd, *J* = 8.6, 2.3 Hz, 1H), 8.84 (s, 1H), 9.87 (d, *J* = 8.6 Hz, 1H), 11.19 (s, 1H); ^{13}C NMR (125 MHz, THF-d_8) δ 10.9, 11.1, 11.8, 20.4, 21.4, 22.0 (2C), 23.2, 27.9, 31.1, 39.5, 39.9, 74.9, 101.9, 114.1, 117.5, 118.0, 123.2, 125.2, 126.9, 127.3, 139.2, 143.4, 143.8, 148.9, 157.6, 162.4, 170.0. Anal. calcd. for $C_{28}H_{34}O_5 \cdot 0.1$EtOAc: C, 74.25; H, 7.64. Found: C, 74.12; H, 7.61.

(*S*)-7-Hydroxy-3-{[2,5,7,8-tetramethyl-2-(4-methylpentyl)chroman-6-yl]oxy}-4*H*-chromen-4-one (14b)

According to the procedure described for the preparation of **1b**, compound **22b** (100 mg, 0.227 mmol) was converted into compound **14b** as white solid (22.7 mg, 22%): mp 255–258 °C; $[\alpha]_D^{25}$ −5.1 (*c* 0.52, THF); IR (neat): 3147 (OH); ^{1}H NMR (500 MHz, THF-d_8) δ 2.69 (d, *J* = 2.9 Hz, 3H), 2.70 (d, *J* = 2.9 Hz, 3H), 3.01 (dd, *J* = 14.9, 6.9 Hz, 2H), 3.06 (s, 3H), 3.26–3.43 (m, 5H), 3.56–3.68 (m, 2H), 3.82 (s, 3H), 3.86 (s, 3H), 3.89 (s, 3H), 4.44 (t, *J* = 6.9 Hz, 2H), 8.47 (d, *J* = 2.3 Hz, 1H), 8.64 (dd, *J* = 8.6, 2.3 Hz, 1H), 8.84 (s, 1H), 9.87 (d, *J* = 8.6 Hz, 1H), 11.20 (s, 1H); ^{13}C NMR (125 MHz, THF-d_8) δ 10.9, 11.1, 11.8, 20.4, 21.4, 22.0 (2C), 23.2, 27.9,

31.1, 39.5, 39.9, 74.9, 101.9, 114.1, 117.5, 118.0, 123.2, 125.2, 126.9, 127.3, 139.2, 143.3, 143.8, 148.9, 157.6, 162.4, 170.0. Anal. calcd. for $C_{28}H_{34}O_5$: C, 74.64; H, 7.61. Found: C, 74.33; H, 7.74.

Screening by the Chemical Array

Photoaffinity linker-coated (PALC) slides were prepared according to previous reports using amine-coated slides and the photoaffinity proline linker [16]. A solution of compounds (2.5 mg/mL in DMSO) from the in-house chemical library (NPDepo, RIKEN) was immobilized onto the PALC glass slides with a chemical arrayer equipped with 24 stamping pins. The slides were exposed to UV irradiation of 4 J/cm^2 at 365 nm using a CL-1000L UV crosslinker (UVP, CA). The slides were washed successively with DMSO, DMF, acetonitrile, THF, dichloromethane, EtOH, and ultra-pure water (5 min, 3 times each), and dried. D- or L-MDM2^{TMR} (3 μM in 1% skim-milk-TBS-T) was incubated with the glass slide for 1 h, and then washed with TBS-T (10 mM Tris-HCl, pH 8.0, 150 mM NaCl, 0.05% Tween-20) (5 min, 3 times). The slides were dried and scanned at 532 nm on a GenePix scanner. The fluorescence signals were quantified with GenePixPro.

FP Assay

FP assays were carried out in PBS containing 2% DMSO and 0.005% Tween-20 using a fluorescein-labeled p53 (P4) peptide (0.5–1.0 nM) and MDM2$^{25-109}$ (10 nM) in black 96-well non-binding surface assay plates (Corning) [16]. The potential inhibitors and FAM-labeled P4 peptide in DMSO were diluted five-fold with PBS in advance. The protein (90 μL) was preincubated with the compound solution (5 μL) for 30 min. Then, the fluorescein-labeled P4 peptide (5 μL) was added and incubated for 30 min. The P4 peptide was used as the positive control. FP signals were analyzed using an EnVision Xcite plate reader (Perkin Elmer) with a 480-nm excitation filter and a 535-nm emission filter.

SPR Analysis

SPR Analyses of p53 binding to synthetic MDM2$^{25-109}$ and MDM2^{TMR} were carried out using Biacore T200 SPR instrument. PBS (Nacalai Tesque, pH 7.4) containing 0.05% Tween-20 was used as the running buffer at 25 °C. Biotinylated wild-type p53 peptides (biotinyl-aminocaproyl-GSGSSQETFSDLWKLLPEN-NH_2) were immobilized on a streptavidin (SA) sensor chip (L-p53: 45.1 RU, D-p53: 46.4 RU). All analytes were evaluated for 2 min as contact time, followed by 2 min dissociation at a flow rate of 30 μL/min.

For competitive inhibition assays, L-MDM2$^{25-109}$ (30 nM) in the presence of varying concentration of inhibitors in PBS containing 0.05% Tween-20 and 1% DMSO were injected on SA sensor chip, where biotinylated wild-type L-p53 peptide was immobilized (127.3 RU).

Competitive Binding Inhibition Assay by a Standard ELISA

ELISA assays were carried out in HEPES buffer [20 mM HEPES (pH 7.4), 100 mM NaCl, 0.05% Tween-20, 0.1% BSA]. Precoated streptavidin 96-well plates (Nunc) were incubated with 300 μL/well of HEPES buffer containing 3% BSA for 1 h. After three washes, biotinylated wild-type p53 peptide (100 nM) in HEPES buffer

(100 μL/well) was added and incubated for 2 h. After three washes, 100 nM MDM2 (recombinant human MDM2, untagged, Sigma) in the presence of varying concentration of inhibitors in HEPES buffer containing 1% DMSO (100 μL/well) was added and incubated for 1 h. After three washes, 1:1000 dilution of anti-MDM2 rabbit IgG antibody (N-20, Santa Cruz] in HEPES buffer (100 μL/well) was added and incubated for 1 h. After three washes, 1:5000 dilution of HRP-conjugated anti-rabbit IgG antibody (Promega) in HEPES buffer (100 μL/well) was added and incubated for 1 h. After three washes, TMB (3,3′,5,5′-Tetramethylbenzidine) solution (WAKO, 100 μL/well) was added and incubated for 1 h. Then, aqueous 2N H_2SO_4 (10 μL/well) was added. Absorbance at 450 nm was measured for each well using an EnVision Xcite plate reader. The IC_{50} values were calculated by using GraphPad Prizm (GraphPad software, San Diego, CA).

Cell Growth Inhibition Assay

SJSA-1 and H1299 cells were cultured in RPMI-1640 medium (high glucose) (WAKO) supplemented with 10% (v/v) FBS at 37 °C in a 5% CO_2-incubator. Cell-based assays using SJSA-1 and H1299 cells were performed in 96-well plates (BD Falcon). Both cells were seeded at 500 cells/well in 50 μL of DMEM, and placed for 6 h. Chemical compounds in DMSO were diluted 250-fold with the culture medium in advance. Following the addition of the fresh culture medium (40 μL), the chemical diluents (30 μL) were also added to the cell cultures. The final volume of DMSO in the medium was equal to 0.1% (v/v). The cells under chemical treatment were incubated for a further 72 h. The wells in the plates were washed with the cultured medium without phenol-red twice. After 1 h of incubation with 100 μL of the medium, the cell culture in each well was supplemented with the MTS reagent (20 μL, Promega), followed by incubation for an additional 40 min. Absorbance at 490 nm was measured for each well using an EnVision Xcite plate reader. The GI_{50} values were calculated by using GraphPad Prizm (GraphPad software, San Diego, CA).

References

1. (a) Toledo F, Wahl GM (2006) Regulating the p53 pathway: in vitro hypotheses, in vivo veritas. Nat Rev Cancer 6:909–923; (b) Wade M, Wang YV, Wahl GM (2010) The p53 orchestra: Mdm2 and Mdmx set the tone. Trends Cell Biol 20:299–309
2. (a) Cahilly-Snyder L, Yang-Feng T, Francke U, George DLS (1987) Molecular analysis and chromosomal mapping of amplified genes isolated from a transformed mouse 3T3 cell line. Cell Mol Genet 13:235–244; (b) Momand J, Zambetti GP, Olson DC, George D, Levine AJ (1992) The mdm-2 oncogene product forms a complex with the p53 protein and inhibits p53-mediated transactivation. Cell 69:1237–1245; (c) Oliner JD, Pietenpol JA, Thiagalingam S, Gyuris J, Kinzler KW, Vogelstein B (1993) Oncoprotein MDM2 conceals the activation domain of tumour suppressor p53. Nature 362:857–860l; (d) Shvarts A, Steegenga WT, Riteco N, van Laar T, Dekker P, Bazuine M, van Ham RC, van der Houven van OW, Hateboer G, van der Eb AJ, Jochemsen AG (1996) MDMX: a novel p53-binding protein with some functional properties of MDM2. EMBO J, 15:5349–5357
3. Honda R, Tanaka H, Yasuda H (1997) Oncoprotein MDM2 is a ubiquitin ligase E3 for tumor suppressor p53. FEBS Lett 22:25–27; (b) Haupt Y, Maya R, Kazaz A, Oren M (1997) Mdm2

promotes the rapid degradation of p53. Nature 387:296–299; (c) Micheal D, Oren M (2003) The p53-Mdm2 module and the ubiquitin system. Semin Cancer Biol 13:49–58; (d) Stommel JM, Wahl GM (2005) A new twist in the feedback loop: stress-activated MDM2 destabilization is required for p53 activation. Cell Cycle 4:411–417
4. Sharp DA, Kratowicz SA, Sank MJ, George DL (1999) Stabilization of the MDM2 oncoprotein by interaction with the structurally related MDMX protein. J Biol Chem 274:38189–38196; (b) Marine JCW, Dyer MA, Jochemsen AG (2007) MDMX: from bench to bedside. J Cell Sci 120:371–378; (c) Wang X (2011) p53 regulation: teamwork between RING domains of Mdm2 and MdmX. Cell Cycle 10:4225–4229; (d) Wang X, Wang J, Jiang X (2011) MdmX protein is essential for Mdm2 protein-mediated p53 polyubiquitination. J Biol Chem 286:23725–23734
5. Wade M, Li YC, Wahl GM (2013) MDM2, MDMX and p53 in oncogenesis and cancer therapy. Nat Rev Cancer 13:83–96
6. Vassilev LT, Vu BT, Graves B, Carvajal D, Podlaski F, Filipovic Z, Kong N, Kammlott U, Lukacs C, Klein C, Fotouhi N, Liu EA (2004) In vivo activation of the p53 pathway by small-molecule antagonists of MDM2. Science 303:844–848
7. Reed D, Shen Y, Shelat AA, Arnold LA, Ferreira AM, Zhu F, Mills N, Smithson DC, Regni CA, Bashford D, Cicero SA, Schulman BA, Jochemsen AG, Guy RK, Dyer MA (2010) Identification and characterization of the first small molecule inhibitor of MDMX. J Biol Chem 285:10786–10796
8. Pazgier M, Liu M, Zou G, Yuan W, Li C, Li C, Li J, Monbo J, Zella D, Tarasov SG, Lu W (2009) Structural basis for high-affinity peptide inhibition of p53 interactions with MDM2 and MDMX. Proc Natl Acad Sci U S A 106:4665–4670
9. Liu M, Pazgier M, Li C, Yuan W, Li C, Lu W (2010) A left-handed solution to peptide inhibition of the p53-MDM2 interaction. Angew Chem Int Ed 49:3649–3652
10. Tsuganezawa K, Nakagawa Y, Kato M, Taruya S, Takahashi F, Endoh M, Utata R, Mori M, Ogawa N, Honma T, Yokoyama S, Hashizume Y, Aoki M, Kasai T, Kigawa T, Kojima H, Okabe T, Nagano T, Tanaka A (2013) A fluorescent-based high-throughput screening assay for small molecules that inhibit the interaction of MdmX with p53. J Biomol Screen 18:191–198
11. Czarna A, Popowicz GM, Pecak A, Wolf S, Dubin G, Holak TA (2009) High affinity interaction of the p53 peptide-analogue with human Mdm2 and Mdmx. Cell Cycle 8:1176–1184
12. Joseph TL, Madhumalar A, Brown CJ, Lane DP, Verma CS (2010) Differential binding of p53 and nutlin to MDM2 and MDMX: computational studies. Cell Cycle 9:1167–1181
13. Hu B, Gilkes DM, Faroogi B, Sebti SM, Chen J (2006) MDMX overexpression prevents p53 activation by the MDM2 inhibitor Nutlin. J Biol Chem 281:33030–33035
14. Danovi D, Meulmeester E, Pasini D, Migliorini D, Capra M, Frenk R, Graaf P, Francoz S, Gasparini P, Gobbi A, Helin K, Pelicci PG, Jochemsen AG, Marine JC (2004) Amplification of Mdmx (or Mdm4) directly contributes to tumor formation by inhibiting p53 tumor suppressor activity. Mol Cell Biol 24:5835–5843
15. Kondoh Y, Honda K, Osada H (2015) Construction and application of a photo-cross-linked chemical array. Methods Mol Biol 1263:29–41
16. Noguchi T, Oishi S, Honda K, Kondoh Y, Saito T, Kubo T, Kaneda M, Ohno H, Osada H, Fujii N (2013) Affinity-based screening of MDM2/MDMX-p53 interaction inhibitors by chemical array: identification of novel peptidic inhibitors. Bioorg Med Chem Lett 23:3802–3805
17. Oliner JD, Kinzler KW, Meltzer PS, George DL, Vogelstein B (1992) Amplification of a gene encoding a p53-associated protein in human sarcomas. Nature 358:80–83
18. Lin DL, Chang C (1996) p53 is a mediator for radiation-repressed human TR2 orphan receptor expression in MCF-7 cells, a new pathway from tumor suppressor to member of the steroid receptor superfamily. J Biol Chem 271:14649–14652
19. (a) Wang P, Dong S, Shieh JH, Peguero E, Hendrickson R, Moore MA, Danishefsky SJ (2013) Erythropoietin derived by chemical synthesis. Science 342:1357–1760; (b) Seenaiah M, Jbara M, Mali SM, Brik A (2015) Convergent versus sequential protein synthesis: the case of ubiquitinated and glycosylated H2B. Angew Chem Int Ed 54:12374–12378
20. Kent SBH, Milton SCF, Milton RCD (1993) D-enzyme compositions and methods of their use. Patent WO 9325667

21. Sankaranarayanan S, Sharma A, Chattopadhyay S (2002) Synthesis of the 1,5-dimethylic chiron enantiomers, 3,7,11-trimethyldodec-10-en-1-ol: application to enantiomeric syntheses of tribolure and a marine fatty acid. Tetrahedron Asymmetry 13:1373–1378
22. Cohen N, Scott CG, Neukom C, Lopresti RJ, Weber G, Saucy G (1981) Total Synthesis of All Eight Stereoisomers of α-Tocopheryl Acetate. Determination of their diastereoisomeric and enantiomeric purity by gas chromatography. Helv Chim Acta 64:1158–1173
23. Muller T, Coowar D, Hanbali M, Heushling P, Luu B (2006) Improved synthesis of tocopherol fatty alcohols and analogs: microglial activation modulators. Tetrahedron 62:12025–12040

http://www.springer.com/978-981-10-6622-1

Development of Chemistry-Based Screening Platform for Access to Mirror-Image Library of Natural Products

Noguchi, T.

2018, XIV, 80 p. 46 illus., 18 illus. in color., Hardcover
ISBN: 978-981-10-6622-1